AD-A136 949 ELECTROCHEMISTRY OF ANILINES II OXIDATION TO DICATIONS 1/1
ELECTROCHEMICAL AN..(U) UTAH UNIV SALT LAKE CITY DEPT
OF CHEMISTRY B SPEISER ET AL. 06 JAN 84 TR-19
UNCLASSIFIED N00014-83-K-0470 F/G 7/4 NL

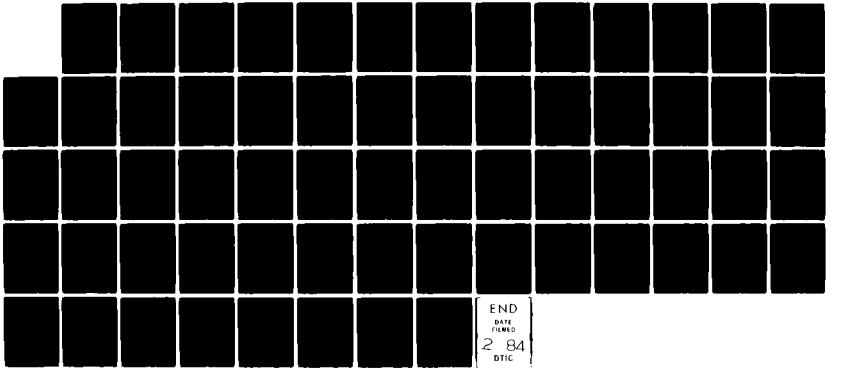

END
DATE FILMED
2 84
DTIC

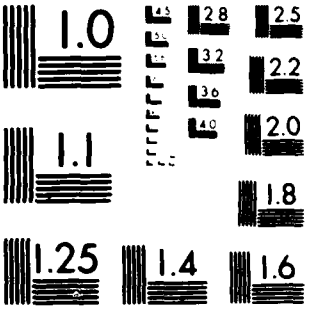

MICROCOPY RESOLUTION TEST CHART
NATIONAL BUREAU OF STANDARDS-1963-A

SECURITY CLASSIFICATION OF THIS PAGE (When Data Entered)

REPORT DOCUMENTATION PAGE

READ INSTRUCTIONS BEFORE COMPLETING FORM

1. REPORT NUMBER: 19	2. GOVT ACCESSION NO.: AD-A136 949
3. RECIPIENT'S CATALOG NUMBER: (12)	
4. TITLE (and Subtitle): Electrochemistry of Anilines II*: Oxidation to Dications, Electrochemical and uv/vis Spectroelectrochemical Investigation	5. TYPE OF REPORT & PERIOD COVERED: Technical Report # 19
	6. PERFORMING ORG. REPORT NUMBER:
7. AUTHOR(s): Bernd Speiser, Anton Rieker, Stanley Pons	8. CONTRACT OR GRANT NUMBER(s): N00014-83-K-0470
9. PERFORMING ORGANIZATION NAME AND ADDRESS: University of Utah, Department of Chemistry, Salt Lake City, UT 84112	10. PROGRAM ELEMENT, PROJECT, TASK AREA & WORK UNIT NUMBERS: Task No. NR 359-718
11. CONTROLLING OFFICE NAME AND ADDRESS: Office of Naval Research, Chemistry Program - Chemistry Code 472, Arlington, Virginia 22217	12. REPORT DATE: January 6, 1984
	13. NUMBER OF PAGES:
14. MONITORING AGENCY NAME & ADDRESS (if different from Controlling Office)	15. SECURITY CLASS. (of this report): Unclassified
	15a. DECLASSIFICATION/DOWNGRADING SCHEDULE

16. DISTRIBUTION STATEMENT (of this Report)

This document has been approved for public release and sale; its distribution unlimited.

17. DISTRIBUTION STATEMENT (of the abstract entered in Block 20, if different from Report)

DTIC ELECTE JAN 19 1984 A

18. SUPPLEMENTARY NOTES

19. KEY WORDS (Continue on reverse side if necessary and identify by block number)

Electrooxidation, Anilines, Spectroelectrochemistry

20. ABSTRACT (Continue on reverse side if necessary and identify by block number)

The electrochemical oxidation of 2,6-di-tert-butyl-4-R-anilines (R = C_2H_5, p-OCH_3-C_6H_4 and p-$N(CH_3)_2$-C_6H_4) at the potentials of the second peak has been investigated. Dications could be observed and characterized by electroanalytical and spectroelectrochemical means. The cyclic voltammogram of the methoxy compound has been simulated by the orthogonal collocation method. Products of bulk electrolysis have been identified. ~~We found~~ two different sites of attack in the case of the methoxy compound were found.

AD A136949

DTIC FILE COPY

DD FORM 1473 84 01 17 121 EDITION OF 1 NOV 65 IS OBSOLETE

S/N 0102-LF-014-6601

Unclassified

SECURITY CLASSIFICATION OF THIS PAGE (When Data Entered)

OFFICE OF NAVAL RESEARCH

Contract N00014-83-K-0470

Task No. NR 359-718

TECHNICAL REPORT NO. 19

Electrochemistry of Anilines II*: Oxidation to Dications, Electrochemical and uv/vis Spectroelectrochemical Investigation

By

Bernd Speiser
Anton Rieker
Stanley Pons*

Prepared for Publication In

Journal of Electroanalytical Chemistry

University of Utah
Department of Chemistry
Salt Lake City, Utah 84112

January 6, 1984

Reproduction in whole or in part is permitted for any purpose of the United States Government

This document has been approved for public release and sale; its distribution is unlimited.

Electrochemistry of Anilines II*: Oxidation to Dications, Electrochemical and uv/vis Spectroelectrochemical Investigation

by

Bernd Speiser[a,b], Anton Rieker[a] and Stanley Pons[b]

a) Institut für Organische Chemie
der Universität Tübingen
Auf der Morgenstelle 18
D-7400 Tübingen-1
Federal Republic of Germany

b) Department of Chemistry
University of Alberta
Edmonton, Alberta, Canada
T6G 2G2

DTIC COPY INSPECTED

Accession For
NTIS GRA&I
DTIC TAB
Unannounced
Justification
Distribution/
Availability Codes
Dist Avail and/or Special
A-1

*part I: see ref. 1

ABSTRACT

The electrochemical oxidation of 2,6-di-tert-butyl-4-R-anilines (R = C_6H_5, p-OCH_3-C_6H_4 and p-$N(CH_3)_2$-C_6H_4) at the potentials of the second peak has been investigated. Dications could be observed and characterized by electroanalytical and spectroelectrochemical means. The cyclic voltammogram of the methoxy compound has been simulated by the orthogonal collocation method. Products of bulk electrolysis have been identified. We found two different sites of attack in the case of the methoxy compound.

INTRODUCTION

In part I of this series on the electrochemistry of anilines [1] we outlined a general scheme for the oxidation of anilines and reported on the electrochemical oxidation of sterically hindered anilines 1a-d to the corresponding radical cations 2a-d* in a first oxidation peak.

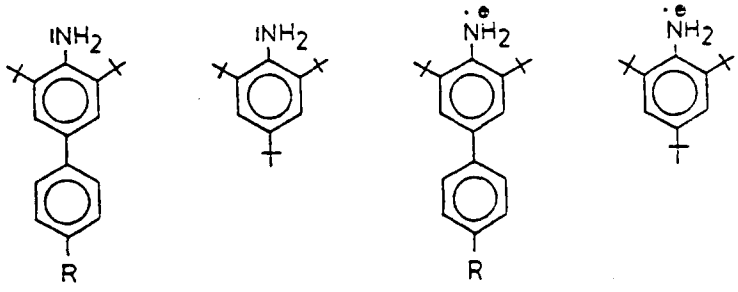

1a : R = H
b : R = OCH_3
c : R = $N(CH_3)_2$

1d

2a : R = H
b : R = OCH_3
c : R = $N(CH_3)_2$

2d

The radical cations 2a-c have been shown to be persistent in the time frame of electroanalytical techniques (chronoamperometry, chronopotentiometry and cyclic voltammetry). These species also have been investigated by uv/vis modulated specular reflectance spectroscopy (MSRS). Spectra as well as transients have been recorded. Both transients and open circuit relaxation experiments showed the persistance of 2a-c and the slow decay of 2d.

---

*We formulate intermediate species in this paper with charges and odd electrons localized at the nitrogen atom. The exact electronic structure of these compounds, however, is not known. Our formulation thus does not imply such a localization.

It has already been mentioned in part 1, that anilines 1a-c show a second oxidation peak at higher potential [1]. Earlier reports on the electrochemistry of 1d [2-4] dealing only with the first oxidation wave of 1d, revealed, however, a small wave at higher potential in rotating disc (RDE) curves [4]. We could detect only a very small peak close to the background oxidation.

In part II of our series on the electrochemistry of anilines, we discuss the anodic oxidation of 1a-c in the second wave investigated by the above mentioned electroanalytical techniques and uv/vis MSRS. We also describe the differences in the mechanisms of the three compounds giving rise to the different patterns revealed in a most obvious way by cyclic voltammetry and the products of bulk electrolyses. We did not investigate the oxidation of 1d in this second wave because of the reason mentioned above.

THE OVERALL VOLTAMMOGRAMS OF ANILINES 1a-c

Typical cyclic voltammograms of the anilines 1a-c at platinum in acetonitrile covering the potential range of both oxidation waves are given in Figures 1a-c. Peaks I and II in all voltammograms correspond to a reversible one-electron transfer to give the radical cations 2. All three compounds show a second oxidation peak III at higher potential. During the second part of the potential scan cycle, however, differences occur. While 1a exhibits no additional reduction peaks, there is one peak IV in the case of aniline 1c. Depending on the experimental conditions we observe one or two peaks IV and V in the case of

1b. These differences must be associated with the different stability of the intermediates produced in the second oxidation wave of the anilines.

ELECTROANALYTICAL EXPERIMENTS WITH 1c

Cyclic voltammetric data for 1c are collected in Table 1. All values are independent of the concentration c and scan rate v.

The difference of peak potentials in cyclic voltammetry $\Delta E_p^{III/IV}$ indicates that the radical cation 2c is further oxidized in a second reversible one-electron step. The peak currents have not been evaluated, because the two formal potentials are very close and it proved very difficult to establish the base line for the second oxidation peak. Figure 1c, however, shows a simulated cyclic voltammetric curve for an EE mechanism with two reversible one-electron transfers which matches the experimental voltammogram very closely. The simulation was performed using the orthogonal collocation technique and our program CYCVOLT.

The ratio of the chronoamperometric constants $(it^{1/2})$ (-0.35 → +0.85 V)/$(it^{1/2})$ (-0.35 → +0.45 V) is 2.0 ± 0.4. We may conclude from this that the number of electrons transferred in going from 1c to the product of the second wave is twice the number of electrons transferred in going from 1c to 2c. Since 2c is a one-electron oxidation product, the product of the second step has to be a two-electron oxidation product.

This is confirmed by chronopotentiometry. The ratio of the

transition times τ_2/τ_1 for the two waves is 3.1 ± 0.2. The theory of this electroanalytical technique [5] shows that for an EE process

$$\frac{\tau_2}{\tau_1} = \frac{(n_1 + n_2)^2 - n_1^2}{n_1^2} \qquad (1)$$

where n_1 and n_2 are the numbers of electrons transferred in the first and second step, respectively. This ratio can only be 3 if $n_1 = n_2 = 1$.

Thus, aniline 1c is oxidized in 2 successive reversible one-electron steps via the radical cation 2c to a species which may be formulated as dication 3c.

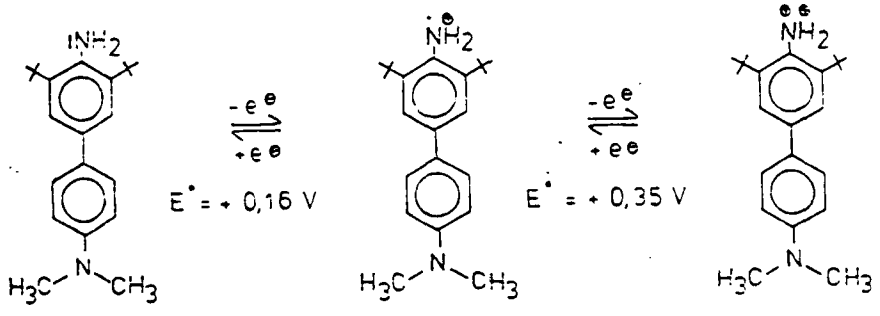

This result may be confirmed by a bulk electrolysis experiment: aniline 1c is oxidized at +0.65 V. After passing of 2.06 Faradays/mol the current has decreased to the background value and the solution has taken on a yellowish brown color. If we reduce this solution at -0.05 V we recover 82% of the aniline after passing 92% of the charge used during oxidation. Thus, the

process 1c ⇌ 3c is also reversible in the time scale of this bulk electrolysis experiment.

Electroanalytical experiments with solutions of 3c prepared in this way show two reversible reductions with E° = +0.34 V and +0.13 V in good agreement with the values resulting from experiments with 1c (Table 1 and [1]). Peak current data, chronoamperometric and chronopotentiometric results prove that 3c is reduced in two one-electron steps, if we assume that all the aniline 1c has been oxidized to the dication 3c and that the diffusion coefficients of aniline and dication are the same.

Serve [6] showed that diarylamines can be oxidized to dications by $SbCl_5$. Aniline 1c has been oxidized by adding this agent, yielding a yellowish brown solution which has the same electroanalytical characteristics as a solution of 3c prepared in the electrochemical way described above. This result also can be achieved using $I_2/AgClO_4$ as oxidizing reagent, while anilines 1a and 1b are oxidized only to the oxidation stage of the radical cation, 2a and 2b resp., by this mixture [1]. This difference may be explained by the low oxidation potential and the small separation between the two formal potentials.

ELECTROANALYTICAL EXPERIMENTS WITH 1b

Cyclic voltammograms of aniline 1b in acetonitrile on platinum are given in Figures 1b and 2. As the disappearance of peak IV and the appearance of peak V at small scan rates v shows, the product of the second oxidation wave undergoes a relatively slow chemical reaction. Quantitative data derived from cyclic

voltammograms are listed in Table 1. The peak separation $\Delta E_p^{III/IV}$ indicates that the radical cation 2b is oxidized in a one-electron step. Obviously, we observe an EEC-mechanism, where the oxidation of 1b yields 3b via the corresponding radical cation 2b:

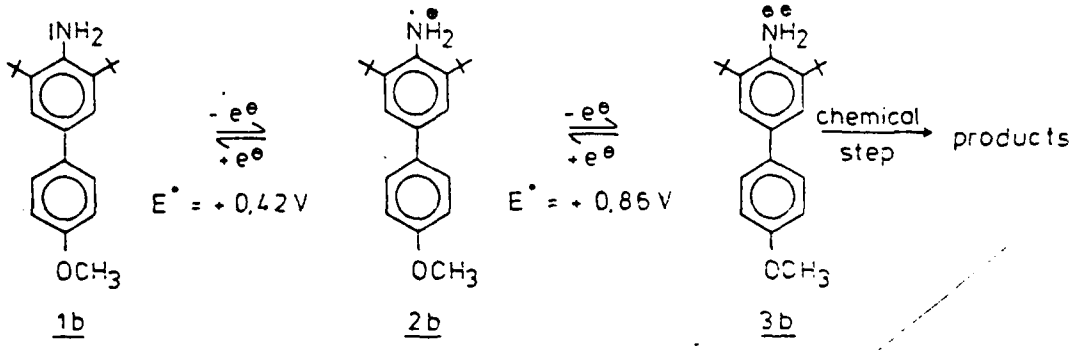

1b 2b 3b

Again, as in the case of 1c, the chronoamperometric constant for a step into the second wave is twice as high as for a step into the first wave. Also, the ratio of the transition times τ_2/τ_1 is near the theoretical value of three for two successive one-electron steps.

That the aniline dication 3b is produced in the second wave can be shown by adding $SbCl_5$ to the solution of 1b and recording voltammograms in the region +1.15 to +0.75 V (where the background current due to $SbCl_5$ reduction increases steeply): peaks IV and III show up.

If we investigate the oxidation of the chemically prepared [1] radical cation 2b, we find n = 1.12 ± 0.07 from chronoamperometry for its oxidation, assuming D (1b) = D (2b).

A quantitative analysis of the peak current data of peaks III and IV has not been attempted, because the actual mechanism is far more complicated than expected from the EEC scheme, as will be shown below. Thus, a determination of the rate constant for this step from cyclic voltammetric data is not possible.

In CH_2Cl_2 as solvent with TEAP as supporting electrolyte, peak IV can be seen even at scan rates where it can not be observed in acetonitrile (v = 0.05 V/s; see Figure 3, compar Figure 2a): the product of the second oxidation wave is mo: persistent in dichloromethane than in acetonitrile. We forr ate the hypothesis that the follow-up reaction of 3b is a deprotonation, which may be faster in acetonitrile because of its slightly basic properties. Dichloromethane should not be able to act as a base.

A close inspection of the voltammograms of 1b in CH_3CN leads to the following questions:

Why is peak II so much smaller when $E_\lambda > E_p^{III}$ compared to $E_p^{I} < E_\lambda < E_p^{III}$ (Figure 1b)?

Why does the current at v = 0.01 V/s during the second part of the cycle go to zero and exhibit a "pseudo" peak (Figure 2b), resembling the behaviour due to proton barrier effects described for 2,6-di-tert-butyl-4-(4-dimethylaminophenyl)-phenol earlier [7]?

As for the peak height of peak II, one could argue that 2b is oxidized in peak III and thus with $E_\lambda > E_p^{III}$ less radical cation is in the vicinity of the electrode to be reduced. A comparison of the experimental voltammogram of 1b and simulated

voltammograms of the reversible one-electron transfer and the EEC mechanism (Figure 4), however, shows that this effect does not totally account for the very small peak current. Although in the case of the EEC mechanism the product of the first electron transfer is irreversibly consumed in the second oxidation wave, it is produced during the second part of the cycle between E^{o}_{2} and E^{o}_{1}. Since we would have to add the base line given by the current of peak V, peak II in an EEC mechanism should not decrease compared to voltammograms with E_{λ} = +0.65 V.

Because 2b is stable on the time scale of voltammetry, we have to assume that at potentials positive of peak III a chemical reaction is triggered which removes 2b or prevents 2b from being produced for a certain time during the second part of the cycle.

Peak II increases if the scan is stopped at a potential between peaks IV and II on the second part of a cycle and restarted after a period of electrolysis at this potential (Figure 5). This strongly supports the hypothesis that 2b is prevented from being produced.

We can show the reason for the observed effect if we add the protonated form of 1b, anilinium cation 7b (we keep the numbering of compounds consistent with part I [1]), to a solution of 1b. We now record the voltammogram given in Figure 6. Compared to voltammograms of 1b alone, we find several differences. Peak III increases considerably, peak II disappears and only peak V can be seen during the second part of the first cycle (peak IV is absent because of the slower scan rate compared to the voltammogram in Figure 1b). In the second cycle, peak I almost disappeares.

This behavior is easily explained by the following mechanism: the anilinium cation 7b is oxidized at potentials similar to those where the oxidation of 2b takes place (peak III). It can be shown [8] that the products of the anilinium cation oxidation are the dication 3b and nitrenium ion 6b, where one or two protons per oxidized molecule are released. The protons are picked up by the basic amino group of aniline 1b, producing more anilinium cation. While scanning the potential positive of peak III, anilinium cation 7b is regenerated in a catalytic mechanism. The ongoing oxidation of 7b produces a large number of protons which diffuse from the electrode out into the solution. Here they encounter aniline molecules and protonate these. Eventually all the aniline in the vicinity of the electrode is transformed into 7b. While scanning back to reach potentials more negative than peak III, the anilinium cation is no longer oxidized. In the vicinity of the electrode, no 1b and thus no oxidizable species is present. As the decrease of peak I in the second cycle shows, the concentration of 1b near the electrode has been depleated considerably.

Let us now return to the voltammograms of 1b alone. We already showed that the decay of dication 3b probably produces protons. These react with 1b, yielding 7b. At the potentials of peak III this compound is oxidized, starting the catalytic cycle discussed above for the mixture of 1b and 7b. Thus, we reduce the amount of 1b near the electrode. Figure 2b shows that the current at this point of the voltammogram drops to zero very fast - before going into the cathodic domain (peaks V and II). As a

further result peak II becomes smaller because the protonation of 1b prevents its oxidation to 2b. Less radical cation is present in the vicinity of the electrode when the potential is negative enough to reduce 2b to 1b in peak II.

The mechanism discussed here also explains why we can see aniline 1b penetrating the "proton barrier" at low scan rates and observe a "pseudo" peak. All features necessary to exhibit this behavior [7] are met: the protonated aniline 7b is oxidizable at a more positive potential than 1b, the species which causes the barrier (H^+) is produced in this second oxidation and because of the "catalytic" regeneration of 7b a large amount of protons is generated while oxidizing at this potential. Thus, the diffusion of 1b to the electrode is totally depressed and the current shows the behavior expected.

The voltammogram in Figure 2b shows this nicely: a comparison of the region marked with an arrow to the corresponding part in our earlier paper [7] supports this conclusion. This is another example of a mechanism where a reaction product prevents the substrate from being oxidized by means of a diffusion process and a chemical reaction.

Now we have to identify the compound which is reduced in peak V. This species must have been produced in the chemical step in which the dication 3b decays. It also undergoes a chemical reaction itself, as shown by voltammograms at low scan rates (e.g. v = 0.01 V/s, Figure 2b): no peak V shows up if the time scale of the experiment is slow.

If 3b deprotonates, we expect nitrenium ion 6b to be

We also observe peaks III and VI in these voltammograms. Peak III corresponds to the oxidation of radical cation 2b, which has been produced by reduction of 3b in peak IV. Peak VI increases if anilinium cation 7b is added to the solution. Obviously, in the presence of acid the oxidation of this species is shifted to higher potential, thus giving rise to a peak separate from peak III.

There are two possible ways by which 7b may be produced:

a) by reduction of 2b to aniline 1b and protonation (reaction path on the right hand side of the scheme). By the follow-up reaction this reduction could be shifted to higher potentials than peak II in voltammograms of 1b.

b) by reduction of nitrenium ion 6b to nitryl radical 5b and a following disproportionation reaction under the influence of protons giving 1b and 6b (which may be reduced again; reaction path on the left hand side of the scheme). Aniline 1b is protonated to give 7b. It is well known that the oxygen analogs of nitryl radical 5 (phenoxy radicals) disproportionate when treated with acid [10].

We could not distinguish between these two possibilities and both have to be taken into account.

At very low scan rates peak V disappears. Nitrenium ion 6b reacts in a chemical reaction. Bulk electrolysis of 1b in the presence of water and 2,6-lutidine shows that iminoquinole 11b is formed. Also, other nucleophiles could be added. A more detailed description of these experiments is in preparation [8]. In the

formed. In analogy to the synthesis of the phenoxenium ion 9 from quinol 10 [9],

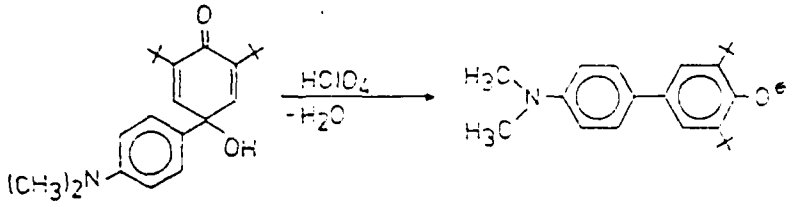

10 9

we tried to generate 6b from the iminoquinol 11b. Voltammograms recorded in solutions of 11b after addition of tetrafluoroboric acid show two reduction peaks whose relative heights depend on the amount of acid used (Figure 7). At low acid concentrations peak V shows up, while at high concentrations peak IV can be seen and V decreases. Thus, we form 3b and 6b, which are in a proton exchange equilibrium:

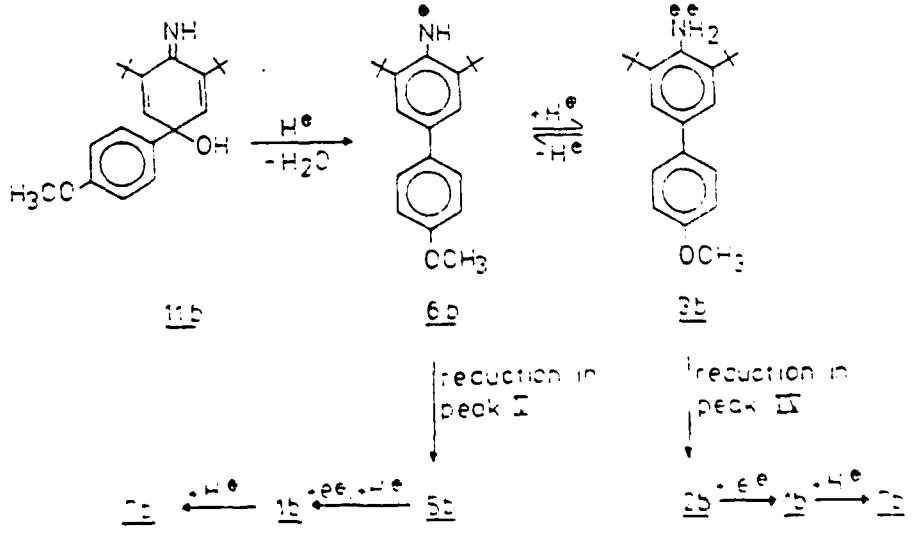

electroanalytical experiments, traces of water are presumably reacting with 6b.

After having established the oxidation mechanism of 1b by electroanalytical methods, we used orthogonal collocation to simulate the model derived from the following reactions under cyclic voltammetric conditions [11,12]:

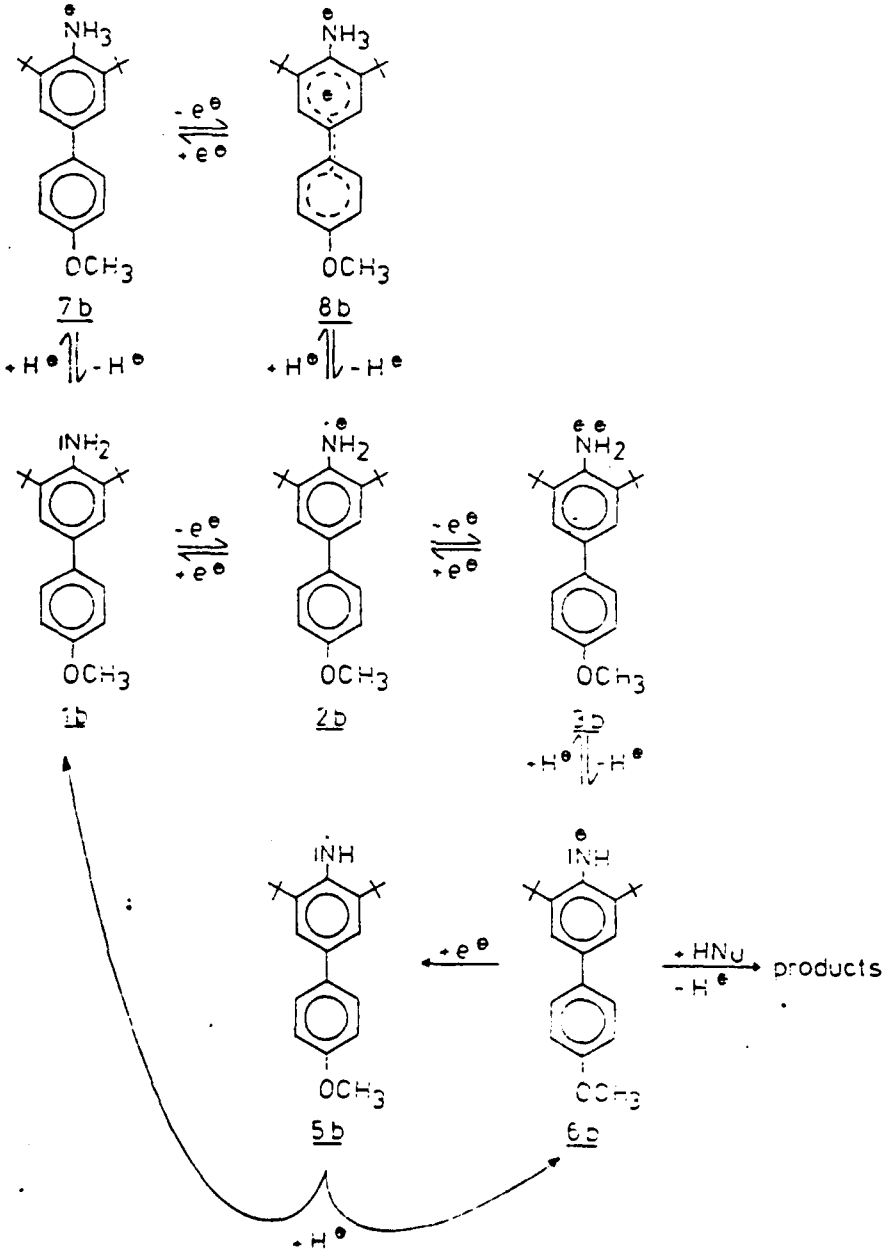

The mathematical equations used are derived in the

Appendix. Figure 8 shows good agreement between simulated and experimental voltammograms for three scan rates (v = 0.1, 0.2 and 0.5 V/s) using the numerical values $E°_{A/B}$ = 0.407 V, $E°_{B/C}$ = 0.818 V, $E°_{HA^+/HA^{\cdot++}}$ = 0.800 V, $E°_{D/E}$ = 0.545 V, k_1 = 1.5 s^{-1}, k_2 = 50 s^{-1}, K_2 = 25, k_3 = 10^4 $l \cdot mol^{-1} \cdot s^{-1}$, k_4 = 0.1 s^{-1}, k_5 = 10^3 $l \cdot mol^{-1} \cdot s^{-1}$, k_6 = 0 s^{-1} (see Appendix for details and symbols).

The value of $E°_{A/B}$ deviates from the numerical value given in ref. [1], because we simulated specific cyclic voltammetric curves while the reported value is a mean value from many experiments. It is problematic to give values for the accuracy of the rate constants derived by this empirical method of comparing experimental and theoretical curves because 11 parameters have an influence on the simulated voltammograms. The good agreement of voltammograms and calculations for three different scan rates, however, shows that at least the order of magnitude should be correct. It also gives support to the proposed mechanism for the oxidation of 1b.

ELECTROANALYTICAL EXPERIMENTS WITH 1a

Cyclic voltammetry of aniline 1a (see Figure 1a) shows that the process occurring in the second peak is not reversible. Even at a scan rate of 50 V/s no reverse peak can be observed. The peak potential varies linearly with ln $v^{1/2}$ (Figure 9), thus indicating that a fast irreversible chemical reaction follows the electron transfer (EC_{irr} mechanism [13]). From the fact that even at 50 V/s no reverse peak is observed, we can conclude that

the rate constant of this follow-up reaction $k > 2000\ s^{-1}$.

In analogy to anilines 1b and 1c we can assume that in this peak radical cation 2a is oxidized to give a dication 3a which deprotonates rapidly. In fact, chemically prepared radical cation 2a shows an oxidation peak near the second peak in the voltammogram of 1a.

The occurrence of a deprotonation step is confirmed by the following observation: reduction peak II is smaller if we pass peak III before switching the potential scan direction. The protons produced by the oxidation of 2a are picked up by as yet unoxidized aniline molecules, thus decreasing the amount of 2a formed while scanning the potential back (see discussion of the mechanism of 1b).

In this case, we do not observe the effect of build up and penetration of a "proton barrier". Because anilinium cation 7a is not oxidized near peak III (addition of acid to a solution of 1a results in the disappearance of all peaks) the blocking protons are not produced in a "catalytic" reaction. Thus, one of the necessary prerequisites [7] to see the diffusion effect is not met.

The chronoamperometric constant for a step to potentials after the second wave is only 10-20% larger than for a step to potentials after the first wave. Since 2a does not react chemically in the time scale of electroanalytical experiments [1], this indicates that 1a must at least partially be removed by protonation. Finally, chronopotentiometric experiments result in a ratio of transition times $\tau_2/\tau_1 < 3$, dependent on the magnitude

of the constant current driven through the electrode, leading to the same conclusion.

The products of the deprotonation reaction of 3a are protonated aniline 7a and nitrenium ion 6a. The anilinium ion 7a is not oxidizable in the potential range investigated (see above). Nitrenium ion 6a could not be detected with electroanalytical methods (see, however, below).

UV/VIS SPECTROELECTROCHEMISTRY* OF 1a - 1c

Uv/vis spectra obtained by the modulated specular reflectance technique (MSR, [15]) are given in Figure 10.

Pulsing the electrode potential from -0.2 to +0.55 V vs the Ag/Ag^+ reference electrode in a solution of 1c produced the spectrum of the dication 3c. The maximum at 4675 Å is shifted only 30 Å from the maximum corresponding to the radical cation 2c at 4645 Å [1]. The band of the dication, however, is narrower than that of the radical cation. The small shift is in accordance with uv/vis spectra obtained from 2c and 3c prepared by chemical oxidation (3c only) and bulk electrolysis (2c and 3c, vide supra, see also ref. [1]). Open circuit relaxation experiments show that the dication is stable on the time scale of the experiments (100 ms - 1 s): no decay can be observed. From the transient obtained by pulsing to +0.55 V we calculate [16] an extinction coefficient of log ε = 4.65 ± 0.01, using the mean

---

*Part of this spectroelectrochemical investigation has been reported as a poster [14].

diffusion coefficient of 1c [1] and assuming that D(1c) = D(3c). Please note that for the calculation of an extinction coefficient equation (17) in reference [16] should read:

$$A(t) = \frac{\Delta R}{R} = 2.303 \cdot \frac{4\varepsilon c (Dt)^{1/2}}{\pi^{1/2} \cos \Theta}$$

Thus, these experiments confirm the conclusion of a reversible electron transfer leading from 1c to 3c.

For the oxidation of 1b in the second peak we observe the MSR spectrum given by the broken line in Figure 10. Both open circuit relaxation and pulse transients show that the absorbing species decays rapidly: when opening the counter electrode circuit, the absorbance curve decays.

The MSR band is broader than the one of 3c. It is shifted to higher wavelength, although one would expect a shift to lower wavelength because the CH_3O-group is less electron-donating than the $(CH_3)_2N$-group. Also, the band exhibits a shoulder on the high wavelength side. This shoulder coincides with the band of the nitrenium ion (5150 Å) [8]. Thus, the band recorded in this experiment may be a superimposition of the dication band and the nitrenium ion band and it seems doubtful whether the maximum at 4850 Å can be assigned to the dication 3b. Further investigations will be reported [8].

Pulsing into the second oxidation wave in the case of aniline 1a, we obtain only a weak spectrum, which shows the two bands of the radical cation and another band at 4525 Å, which can

be identified as due to the nitrenium ion 6a [8]. Thus, we are not able to record the spectrum of dication 3a but can observe the formation of 6a as a product of the second oxidation wave. The weak spectrum may be explained by the fact that all observable species [2a (by further oxidation) and 6a] are reacting fast.

BULK ELECTROLYSES WITH 1a - 1c

The bulk electrolysis experiments with 1c have already been described (vide supra and ref. [1]). The stable species 2c and 3c are the products of the oxidation at the first and second wave, respectively.

Dication 3b reacts chemically, and we find products of this reaction after bulk electrolysis. If we electrolyse 1b at +1.45 V, the solution turns from colourless to green, yellow-green and finally, after 2.5 Faradays/mol have been passed, to a brownish orange. We were not able to isolate products from this mixture. If we reduce the solution at -0.35 V, however, 1.9 Faradays/mol (calculated for 1b) are passed, and we isolate three compounds after preparative TLC: aminophenol 12, o-dihydroxybenzene 13 and benzoxazole 14.

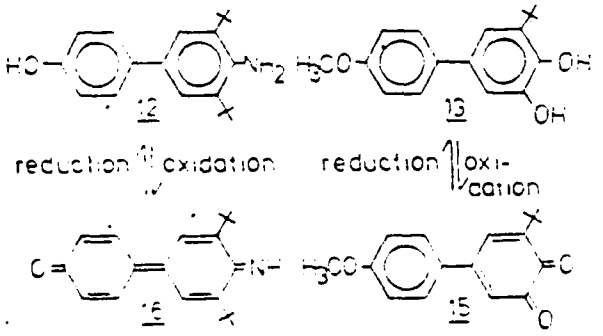

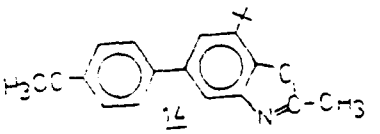

Compounds 12 and 13 may be oxidized by $K_3[Fe(CN)_6]$ to strongly coloured species. The oxidation product of 13 could be shown to be the biphenyl-o-quinone 15 (by comparison to an authentic sample), while 12 is presumably oxidized to quinoneimine 16. Comparison of the R_f values in TLC to the ones of authentic samples suggests that 15 and 16 are present in the brownish orange solution after oxidation of 1b.

The electroanalytical and spectroelectrochemical evidence given in the preceding chapters and ref. [1] has shown that 1b is oxidized to 3b via 2b. Solutions of 2b in acetonitrile are persistent for several hours. Thus, 2b cannot be the reacting species, and the products must be derived from 3b or its follow-up products. We also have shown that the reactions involve deprotonations.

One possibility for the reaction of 1b to 12, 13, and 14 is given in the following scheme.

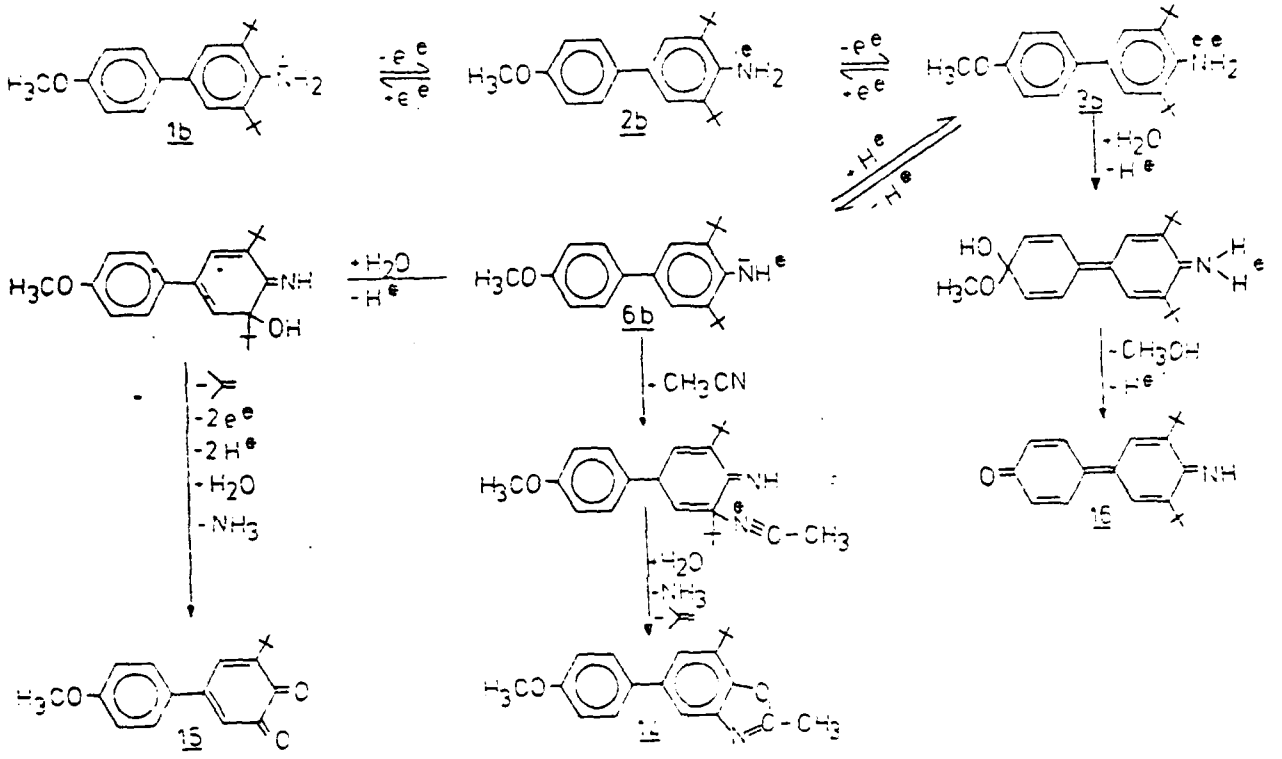

Aniline 1b is oxidized in a two-electron process to give the dication 2b, which is connected with the nitrenium ion 6b via a deprotonation/protonation equilibrium. The nitrenium ion can be attacked by the nucleophiles water or acetonitrile. The cleavage of one of the tert-butyl groups may be facilitated by the presence

of protons in the solution (produced by the deprotonation 3b → 6b). In the case of the water attack, a series of oxidation and hydrolysis reactions finally leads to 15. The acetonitrile adduct, after hydrolysis and ring formation, yields 14. The correct sequence of the individual steps leading from 6b to 15 and 14 is not known.

Iminoquinone 16 seems to have been formed via the attack of water on the dication 3b itself. In this species, the positive charge density in the para-position of the second ring bearing the methoxy group must be considerably larger than in the nitrenium ion 6b. Also, the dication may have the higher energy and may more easily reach a transition state where the aromatic system in both rings has been distorted. Cleavage of the methoxy group as methanol would result in the formation of 16. Oxidative cleavage of aromatic methyl ethers is a well-known reaction [17 - 23].

It is also possible, however, to formulate the reactions leading to 14 and 15 via the dication 3b or to 16 via the nitrenium ion 6b. Also, hydrolysis of the dication itself or the nitrenium ion at the nitrogen moiety may occur to produce the corresponding phenoxenium ion, which could react to give 14 and 15. Analogous reactions of phenoxenium ions with acetonitrile, water, and other nucleophiles have been observed previously [24 - 28].

That 15 and 16 may be reduced at -0.35 V can be shown by cyclic voltammetry of these species, produced by chemical oxidation of 13 and 12. o-Quinone 15 is reduced in two waves at -0.45 V and -1.0 V in neutral solution. Addition of acid shifts these potentials to values positive enough to achieve the reduction at -0.35 V. In the bulk electrolyses, protons are produced during the oxidation step. Compound 16 shows two reduction peaks at +0.5 and -0.45 V in neutral solution. Acid also causes a shift to more positive values.

Bulk electrolysis of 1a results in the formation of iminoquinole 11a with a yield of 40%. Here we only observe the product of water attack on the para-position of the nitrenium ion 6a. The dication 3a decays too fast by deprotonation for

products of its reactions to be formed.

CONCLUSION

Anilines 1a-c are oxidized in two waves to the corresponding dications 3a-c via radical cations 2a-c [1]. The different persistance of the dications gives rise to different responses to electroanalytical and spectroelectrochemical techniques: while 3c is persistent and the oxidation of 1c follows an EE mechanism, 3b decays moderately fast in a complicated reaction and we can observe the reduction of a further intermediate, nitrenium ion 6b. Also, protonation of the parent aniline occurs. Intermediate 3a, however, decays extremely fast and could be detected neither electroanalytically nor spectroelectrochemically.

Bulk electrolysis yields products derived from dications (1b) and/or nitrenium ions (1a, 1b). Starting with 1c the persistent dication 3c is observed.

To our knowledge this is the first reported observation of dications derived from primary aromatic amines.*

EXPERIMENTAL PART

The preparation and purification of the anilines 1a-c, acetonitrile and the supporting electrolytes (TEAP, commercial $NaClO_4$ and $LiClO_4$ have been used after drying) has been described [1]. Dichloromethane was purified by passing through a column of alumina. The electroanalytical techniques were standard, spectroelectrochemical experiments followed the directions

* See, however, the formulation of such dications as mechanistic intermediates in chemical reactions in lit.[29].

outlined in earlier papers [1,15,16]. Potentials were measured vs a saturated calomel electrode or vs an Ag/Ag^+ (0.01 M in CH_3CN) electrode. All potentials in this paper are given vs the latter reference electrode. Values measured with the SCE were converted as described in [1].

Simulations were performed on the TR440 of the Rechenzentrum der Universität Tübingen using the dialogue program CYCVOLT (see Appendix) written in FORTRAN IV.

Mass spectra were taken with AEI MS9 or Varian MAT 711 spectrometers (ionization energy 70 eV). ^{1}H-nmr spectra were recorded with Varian EM360 or Bruker HFX 90 spectrometers (δ-scale, TMS as internal standard).

Oxidation of 1c with $AgClO_4/I_2$

0.05 g (0.15 mmol) of the aniline 1c were dissolved in absolute ether and 0.08 g (0.32 mmol) of I_2 in ether and subsequently 0.12 g (0.58 mmol) of $AgClO_4$ in ether were added. A mixture (0.13 g) of AgI and 3b (as perchlorate) precipitated, was filtered off and washed 3 times with 10 ml of absolute ether. The dication salt could not be separated from AgI.

Electrochemical oxidation of 1c

0.21 g (0.65 mmol) of 1c were dissolved in 200 ml of CH_3CN/0.1 M $NaClO_4$ and oxidized at a Pt anode at +0.65 V. After 129 C have been passed (theoretical for n=2: 125 C) the solution has turned to an orange brown colour. A volume of 25 ml solution was taken out of the cell to record uv/vis spectra and to perform electroanalytical experiments. The remaining dication

was reduced at -0.05 V. Now 104 C (theoretical for n =2: 109 C) could be passed and the solution turned colourless. After evaporation of the solvent, extraction with petroleum ether, and crystallization, 0.15 g (82%) of the aniline 1c could be recovered.

Electrochemical oxidation of 1b

0.25 g (0.80 mmol) of aniline 1b were dissolved in 200 ml of CH_3CN/0.1 M TEAP and oxidized at a Pt anode at +1.45 V. The solution turned purple for a couple of seconds, then green, yellowish green and finally yellowish brown. A charge of 200 C (theoretical for n = 2: 155 C) passed. We could not isolate any products from this solution. Reduction of the products was performed in the same cell at -0.35 V. After passing 150 C the solution had lost its colour and was poured into 1 liter of distilled water. Extraction with ether, drying of the organic phase with Na_2SO_4 and evaporating the solvent yielded an oil, which could be separated into three fractions (12, 13, 14) by TLC (plates made from Macherey and Nagel PUV_{254} silica gel, 20 x 20 cm, layer thickness 2 mm) with petroleum ether/acetone, (5:2), as solvent.

Characterization of 4'-amino-3',5'-di-tert-butyl-biphenyl-4-ol 12 [yield: 50 mg (21%), m.p. 176-178°C (from methanol)]: I.r. (KBr): 3550-3150 (broad, structured band, O-H, N-H), 2960 cm^{-1} (C-H). ^1H-nmr (d^6-acetone): δ = 1.48 (s, 18 H, tert-butyl), 4.37 (s, broad, 2H, NH_2), 7.12 (q, A_2B_2, J ca. 9 Hz) and 7.33 (s) (6H, aromatic protons), 8.16 (s, broad, 1H, disappears after addition of D_2O, OH). M.s.: m/e = 297 (78%; M^+), 282

(100%; M^+-CH_3), 271 (25%). Analysis: $C_{20}H_{27}NO$ (297.4) Calc. C 80.76, H 9.15, N 4.71; Found C 80.58, H 9.15, N 4.83.

Characterization of 5-tert-butyl-4'-methoxy-biphenyl-3,4-diol 13 [yield: 40 mg (18%); m.p.: 128-130° (from petroleum ether with addition of little acetone)]:

I.r. (KBr): 3600-3150 (broad, 2 bands, OH), 2950 (C-H), 1235 cm^{-1} (C-O). ^1H nmr ($CDCl_3$): δ = 1.46 (s, 9H, tert-butyl), 3.84 (s, 3H, OCH_3), 5.64 (s, broad, 2H, OH), 6.98 (q, AB, J ca. 2Hz) and 7.19 (q, A_2B_2, J ca. 9Hz) (6H, aromatic protons). M.s.: m/e = 272 (100%; M^+), 257 (54%; M^+-CH_3). Analysis: $C_{17}H_{20}O_3$ (272.3) Calc. C 74.97, H 7.40; Found C 74.81, H 7.28.

Characterization of 7-tert-butyl-5-(4-methoxyphenyl)-2-methylbenzoxazole 14 [yield: 20 mg (8%); m.p.: 95°C (from petroleum ether)]:

I.r. (KBr): 2960 cm^{-1} (C-H). ^1H nmr ($CDCl_3$): δ = 1.49 (s, 9H, tert-butyl), 2.65 (s, 3H, CH_3), 3.84 (s, 3H, OCH_3), 7.25 (q, A_2B_2, J ca. 9 Hz) and 7.46 (q, AB, J ca. 2 Hz) (aromatic protons). M.s.: m/e = 295 (100%; M^+), 280 (73%; M^+-CH_3). Analysis: $C_{19}H_{21}NO_2$ (295.4) Calc. C 77.26, H 7.17, N 4.74; Found C 77.01, H 7.03, N 4.62.

ACKNOWLEDGEMENTS

We thank the Fonds der Chemischen Industrie for financial support. B.S. wishes to acknowledge scholarships of the Universität Tübingen (during work on the doctoral thesis) and the Killam Foundation of Canada (postdoctoral work). S.P. thanks the Office of Naval Research for support of part of this work.

$$+ \sum_{j=2}^{N+1} B_{i,j} c_E^*(X_j,T')\} - 2\alpha_5 c_E^* c_H^{*+} \qquad (A40)$$

$$\left.\frac{dc_H^{*+}}{dT'}\right|_{X_i} = s\{-\frac{B_{i,1}}{A_{1,1}} \sum_{j=2}^{N+1} A_{1,j} c_H^{*+}(X_j,T') + \sum_{j=2}^{N+1} B_{i,j} c_H^{*+}(X_j,T')\}$$

$$+ \alpha_1 c_C^* - \alpha_2 c_A^* c_H^{*+} + \frac{\alpha_2}{K_2} c_{HA}^{*+} + \alpha_3 c_{HA}^{*\cdot++} - \alpha_5 c_E^* c^*{}_H{}^+ + \alpha_4 c_D^* \qquad (A41)$$

$$\left.\frac{dc_{HA}^{*+}}{dT'}\right|_{X_i} = s\{-\frac{B_{i,1}\Theta_{HA^+/HA\cdot++} S_\lambda(T')}{A_{1,1}[1+\Theta_{HA^+/HA\cdot++} S_\lambda(T')]} \sum_{j=2}^{N+1} A_{1,j}[c_{HA}^{*+}(X_j,T')+c_{HA}^{*\cdot++}(X_j,T')]$$

$$+ \sum_{j=2}^{N+1} B_{i,j} c_{HA}^{*+}(X_j,T')\} + \alpha_2 c_A^* c_H^{*+} - \frac{\alpha_2}{K_2} c_{HA}^{*+} \qquad (A42)$$

$$\left.\frac{dc_{HA}^{*\cdot++}}{dT'}\right|_{X_i} = s\{-\frac{B_{i,1}}{A_{1,1}[1+\Theta_{HA^+/HA\cdot++} S_\lambda(T')]} \sum_{j=2}^{N+1} A_{1,j}[c_{HA}^{*+}(X_j,T')$$

$$+ c_{HA}^{*\cdot++}(X_j,T')] + \sum_{j=2}^{N+1} B_{i,j} c_{HA}^{*\cdot++}(X_j,T')\} - \alpha_3 c_{HA}^{*\cdot++} \qquad (A43)$$

From the concentration profiles generated by solving this system of equations, we can calculate the current function

$$\chi(at) = \sqrt{\frac{\xi}{\pi}}\{[1 - \frac{n_2}{n_1}]\{- \frac{\Theta_{A/B}\Theta_{B/C} S_\lambda(T')^2}{[1+\Theta_{B/C} S_\lambda(T') + \Theta_{A/B}\Theta_{B/C} S_\lambda(T')^2]} \times$$

$$\left(A_{1,N+2} + \sum_{j=2}^{N+1} A_{1,j}[c_A^*(X_j,T') + c_B^*(X_j,T') + c_C^*(X_j,T')]\right)$$

$$+ A_{1,N+2} + \sum_{j=2}^{N+1} A_{1,j} c_A^*(X_j,T') - \frac{\Theta_{B/C} S_\lambda(T')}{[1+\Theta_{B/C} S_\lambda(T') + \Theta_{A/B}\Theta_{B/C} S_\lambda(T')^2]} \times$$

$$\left(A_{1,N+2} + \sum_{j=2}^{N+1} A_{1,j}[c_A^*(X_j,T') + c_B^*(X_j,T') + c_C^*(X_j,T')]\right)$$

$$+ \sum_{j=2}^{N+1} A_{1,j} c_B^*(X_j,T')] + \frac{n_3}{n_1}\left[\frac{1}{1+\Theta_{HA^+/HA^{\cdot++}} S_\lambda(T')}\left(\sum_{j=2}^{N+1} A_{1,j} c^*_{HA^+}(X_j,T')\right.\right.$$

$$\left.\left. - \Theta_{HA^+/HA^{\cdot++}} S_\lambda(T') \sum_{j=2}^{N+1} A_{1,j} c^*_{HA^{\cdot++}}(X_j,T')\right)\right]$$

$$- \frac{n_4}{n_1}\left[\frac{1}{1+\Theta_{E/D} S_\lambda(T')}\left(\sum_{j=2}^{N+1} A_{1,j} c_E^*(X_j,T') - \Theta_{E/D} S_\lambda(T') \sum_{j=2}^{N+1} A_{1,j} c_D^*(X_j,T')\right)\right]\right] \tag{A44}$$

As has been shown [12], it is necessary to optimize the value of the dimensionless parameter δ. Using the method given in ref. [12], we arrive at:

$$\frac{0.65 - h\,\alpha_2 c_H^{*+}}{h\left| - \frac{B_{i,1}\theta_{A/B}\theta_{B/C}\,S_\lambda(T')^2}{A_{1,1}[1+\theta_{B/C}S_\lambda(T') + \theta_{A/B}\theta_{B/C}S_\lambda(T')^2]}\,A_{1,i} + B_{i,i}\right|} \qquad i = 2, \ldots, N+1 \qquad \text{(A45a)}$$

$$\frac{0.65 - h\,\alpha_6}{h\left| - \frac{B_{i,1}\theta_{B/C}S_\lambda(T')}{A_{1,1}[1+\theta_{B/C}S_\lambda(T')+\theta_{A/B}\theta_{B/C}S_\lambda(T')^2]}\,A_{1,i}+B_{i,i}\right|} \qquad i=2, \ldots, N+1 \qquad \text{(A45b)}$$

$$\frac{0.65 - h\,\alpha_1}{h\left| - \frac{B_{i,1}}{A_{1,1}[1+\theta_{B/C}S_\lambda(T')+\theta_{A/B}\theta_{B/C}S_\lambda(T')^2]}\,A_{1,i}+B_{i,i}\right|} \qquad i=2, \ldots, N+1 \qquad \text{(A45c)}$$

$$\frac{0.65 - h\,\alpha_4}{h\left| - \frac{B_{i,1}}{A_{1,1}[1+\theta_{E/D}S_\lambda(T')]}\,A_{1,i} + B_{i,i}\right|} \qquad i=2, \ldots, N+1 \qquad \text{(A45d)}$$

$$\frac{0.65 - 2\,h\,\alpha_5 c^*{}_{H^+}}{h\left| - \frac{B_{i,1}\theta_{E/D}S_\lambda(T')}{A_{1,1}[1+\theta_{E/D}S_\lambda(T')]}\,A_{1,i} + B_{i,i}\right|} \qquad i=2, \ldots, N+1 \qquad \text{(A45e)}$$

$$\frac{0.65-h\,\alpha_2 c_A^* - h\,\alpha_5 c_E^*}{h\left| - \frac{B_{i,1}}{A_{1,1}}\,A_{1,i} + B_{i,i}\right|} \qquad i=2, \ldots, N+1 \qquad \text{(A45f)}$$

$$\frac{0.65 - h\,\alpha_2/K_2}{h\left| - \frac{B_{i,1}\theta_{HA^+/HA^{\cdot++}}\,S_\lambda(T')}{A_{1,1}[1-\theta_{HA^+/HA^{\cdot++}}\,S_\lambda(T')]}\,A_{1,i} + B_{i,i}\right|} \qquad i=2, \ldots, N+1 \qquad \text{(A45g)}$$

$$\frac{0.65 - h\,\alpha_3}{h\left| - \frac{B_{i,1}}{A_{1,1}[1+\Theta_{HA^+/HA^{\cdot}}{}^{++}\, S_\lambda(T')]}\, A_{1,i} + B_{i,i}\right|} \qquad i=2, \ldots, N+1 \qquad \text{(A45h)}$$

where h is the integration stepwidth.

We used the dialogue program CYCVOLT (a list of FORTRAN statements and a program description is available from B.S.) to solve the system of equations (A36)-(A43) and generate theoretical voltammograms.

REFERENCES

1. B. Speiser, A. Rieker and S. Pons, J. Electroanal. Chem., in press.
2. G. Cauquis, G. Fauvelot and J. Rigaudy, C.R. Acad. Sci. Paris, 264 (1967) 1758.
3. G. Cauquis, G. Fauvelot and J. Rigaudy, C.R. Acad. Sci. Paris, 264 (1967) 1958.
4. G. Cauquis, G. Fauvelot and J. Rigaudy, Bull. Soc. Chim. France (1968) 4928.
5. D.D. McDonald, Transient Techniques in Electrochemistry, Plenum Press, New York, London, p. 126.
6. D. Serve, J. Am. Chem. Soc., 97 (1975) 432.
7. B. Speiser and A. Rieker, Electrochim. Acta, 23 (1978) 983.
8. B. Speiser, A. Rieker, S. Pons, et al. in preparation; see also B. Speiser, Dissertation, Universität Tübingen, 1981.
9. B. Speiser and A. Rieker, J. Chem. Res. (S), (1977) 314.
10. W.A. Waters, J. Chem. Soc. (B), (1971) 2026.
11. B. Speiser and A. Rieker, J. Electroanal. Chem., 102 (1979) 1.
12. B. Speiser, J. Electroanal. Chem., 110 (1980) 69.
13. R.S. Nicholson and I. Shain, Anal. Chem., 36 (1964) 706.
14. B. Speiser, S. Pons, and T.M. Davidson, "Spectroelectrochemistry of sterically hindered anilines", Poster at the 33rd ISE meeting, Lyon/France, September 1982; extended abstracts, p. 677.
15. S. Pons and S.B. Khoo, J. Am. Chem. Soc., 104 (1982) 3845.
16. A. Bewick, J.M. Mellor and B.S. Pons, Electrochim. Acta, 25

(1980) 931.

17. A. Nilsson, U. Palmquist, A. Ronlán and V.D. Parker, J. Am. Chem. Soc., 97 (1975) 3540.
18. W.E. Britton and C. Steelink, Tetrahedron Lett., (1974) 2873.
19. D.W. Leedy, J. Electroanal. Chem. Interfac. Electrochem., 45 (1973) 467.
20. M. Petek, S. Brukenstein, B. Feinberg and R.N. Adams, J. Electroanal. Chem. Interfac. Electrochem., 42 (1973) 397.
21. D.W. Leedy and R.N. Adams, J. Am. Chem. Soc., 92 (1970) 1646.
22. D. Serve, Nouv. J. Chim., 4 (1980) 497.
23. G. Cauquis, H. Delhomme and D. Serve, Electrochim. Acta, 21 (1976) 557.
24. A.B. Suttie, Tetrahedron Lett., (1969) 953.
25. A. Rieker, Tetrahedron Lett., (1969) 2611.
26. E.L. Dreher, J. Bracht, M. El-Nobayed, P. Hütter, W. Winter and A. Rieker, Chem. Ber. 115 (1982) 288.
27. A. Rieker, E.L. Dreher, H. Geisel and M.H. Khalifa, Synthesis, (1978) 851.
28. M.H. Khalifa, G. Jung and A. Rieker, Liebigs Ann. Chem. (1982) 1068.
29. H. Shudo, T. Ohta and T. Okamoto, J. Am. Chem. Soc., 103 (1981) 645.

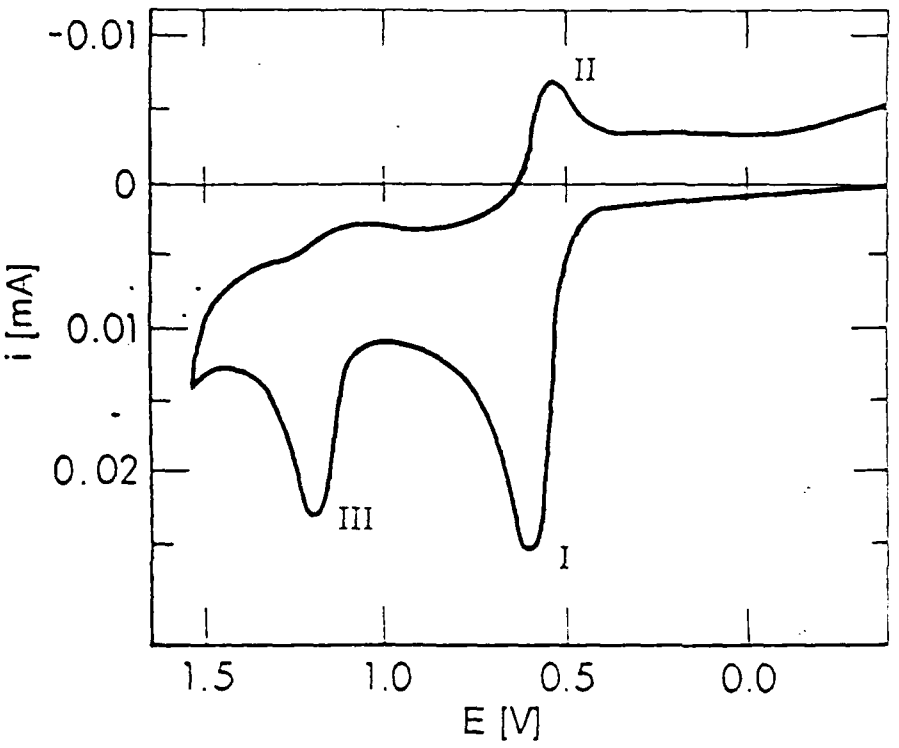
-0.01
0
0.01
0.02
i [mA]
II
III
I
1.5
1.0
0.5
0.0
E [V]

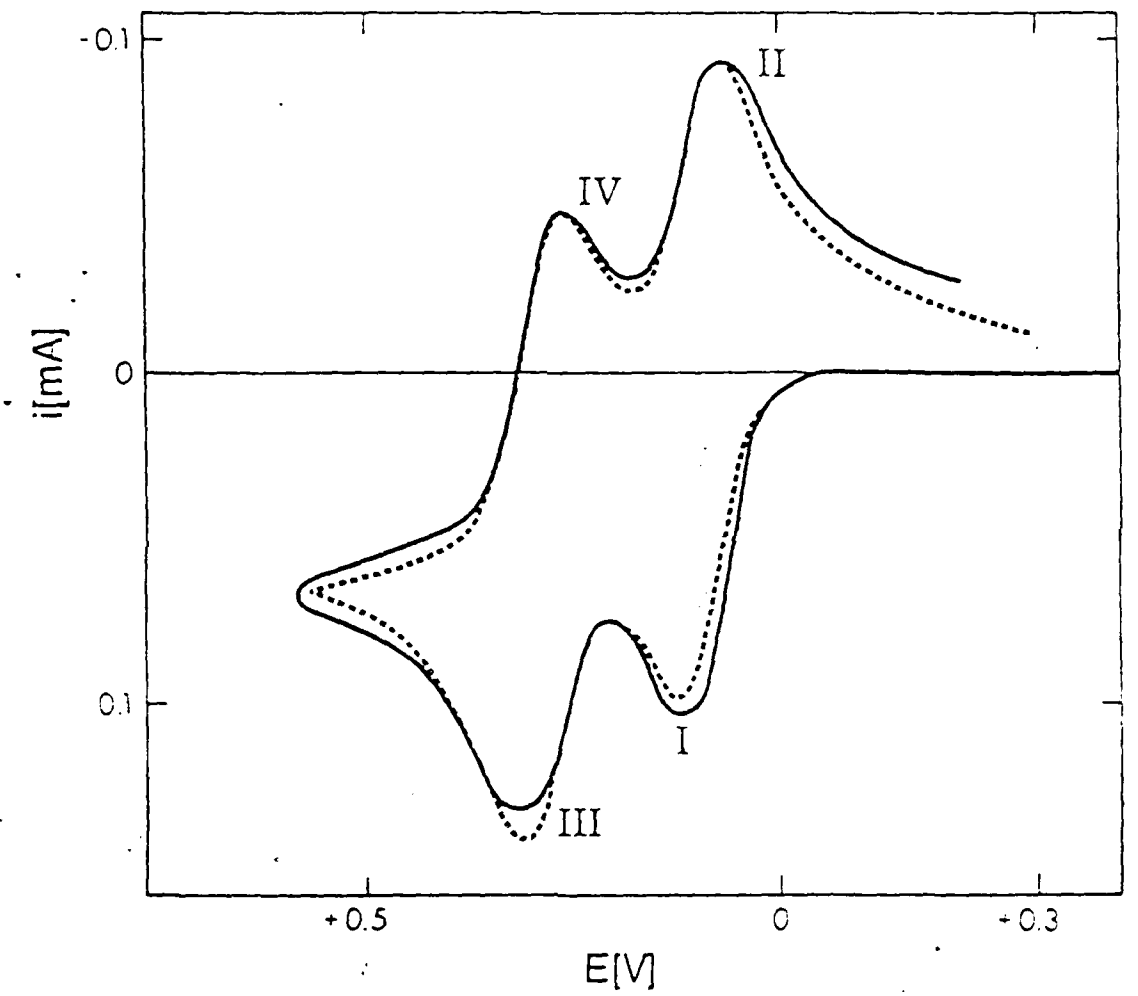
-0.1
0
0.1
i[mA]
II
IV
I
III
+0.5
0
+0.3
E[V]

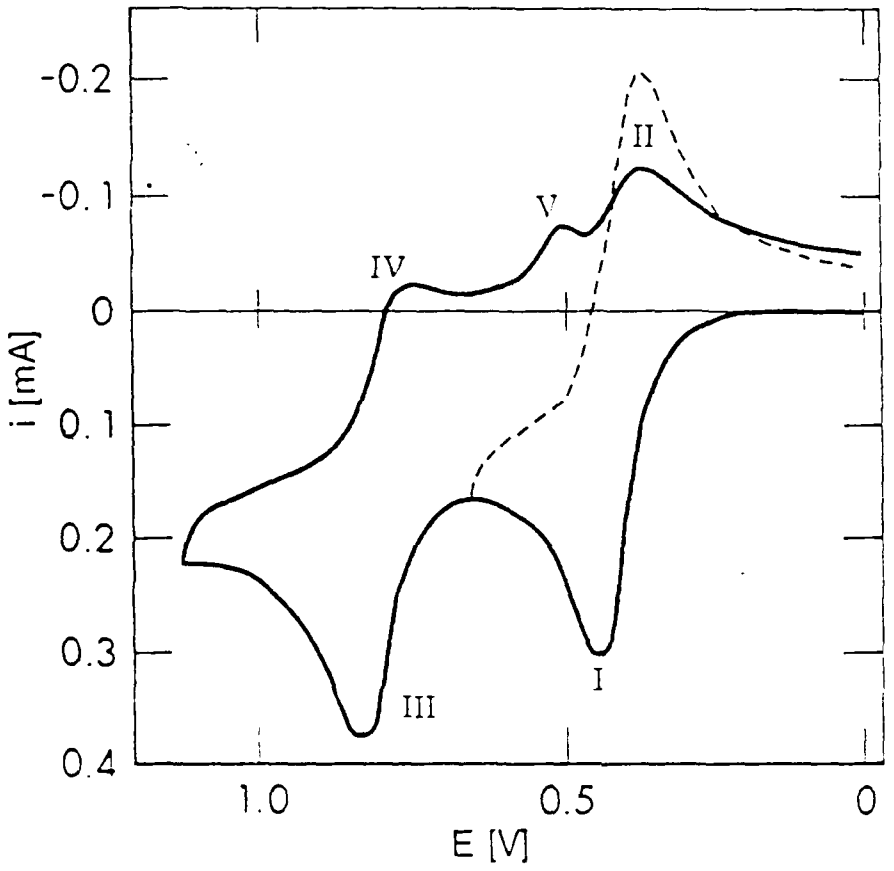
-0.2
-0.1
0
0.1
0.2
0.3
0.4
i [mA]
1.0
0.5
0
E [V]
I
II
III
IV
V

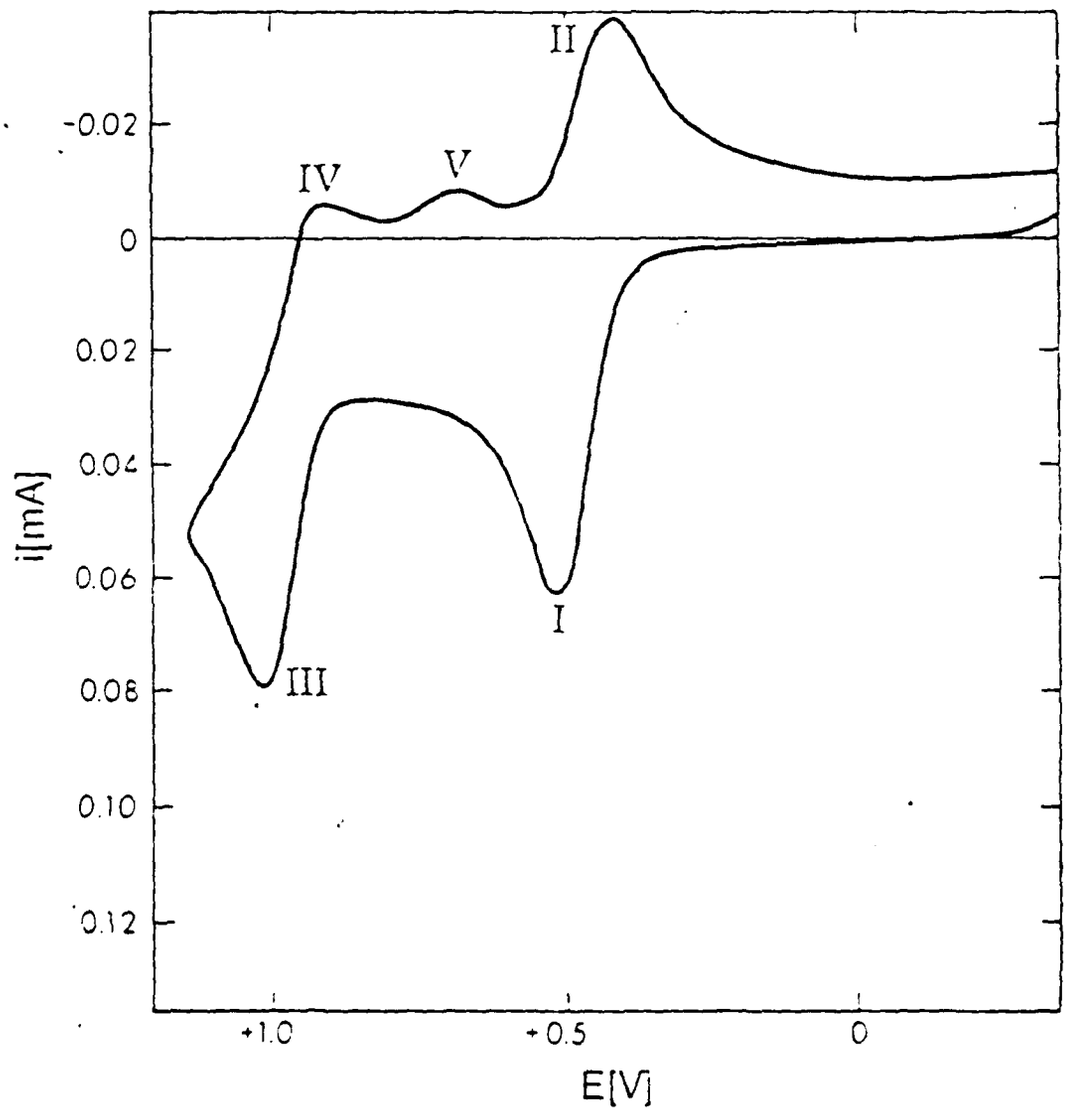
II
IV
V
I
III
-0.02
0
0.02
0.04
0.06
0.08
0.10
0.12
i[mA]
+1.0
+0.5
0
E[V]

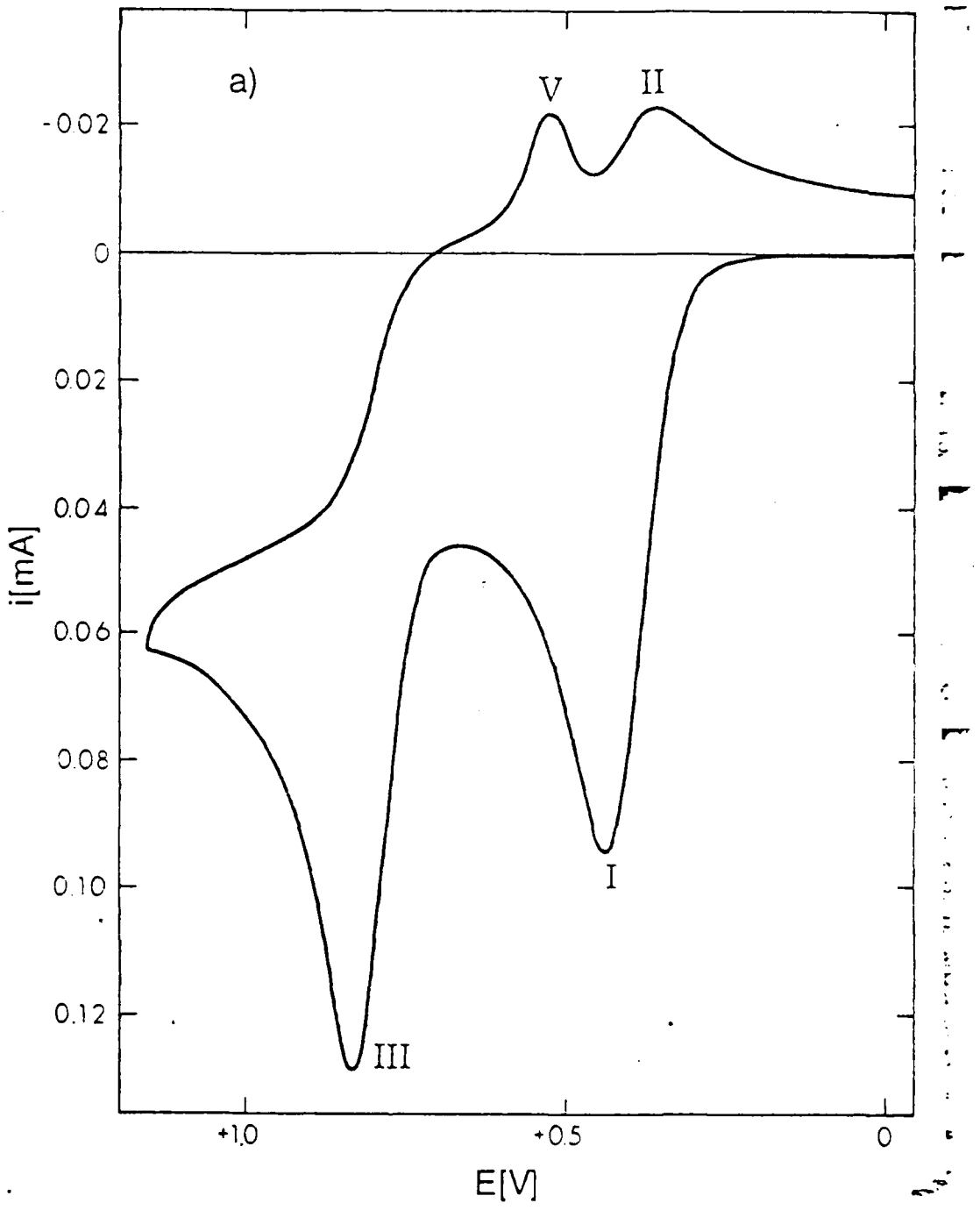
a)
V
II
I
III
-0.02
0
0.02
0.04
0.06
0.08
0.10
0.12
i[mA]
+1.0
+0.5
0
E[V]

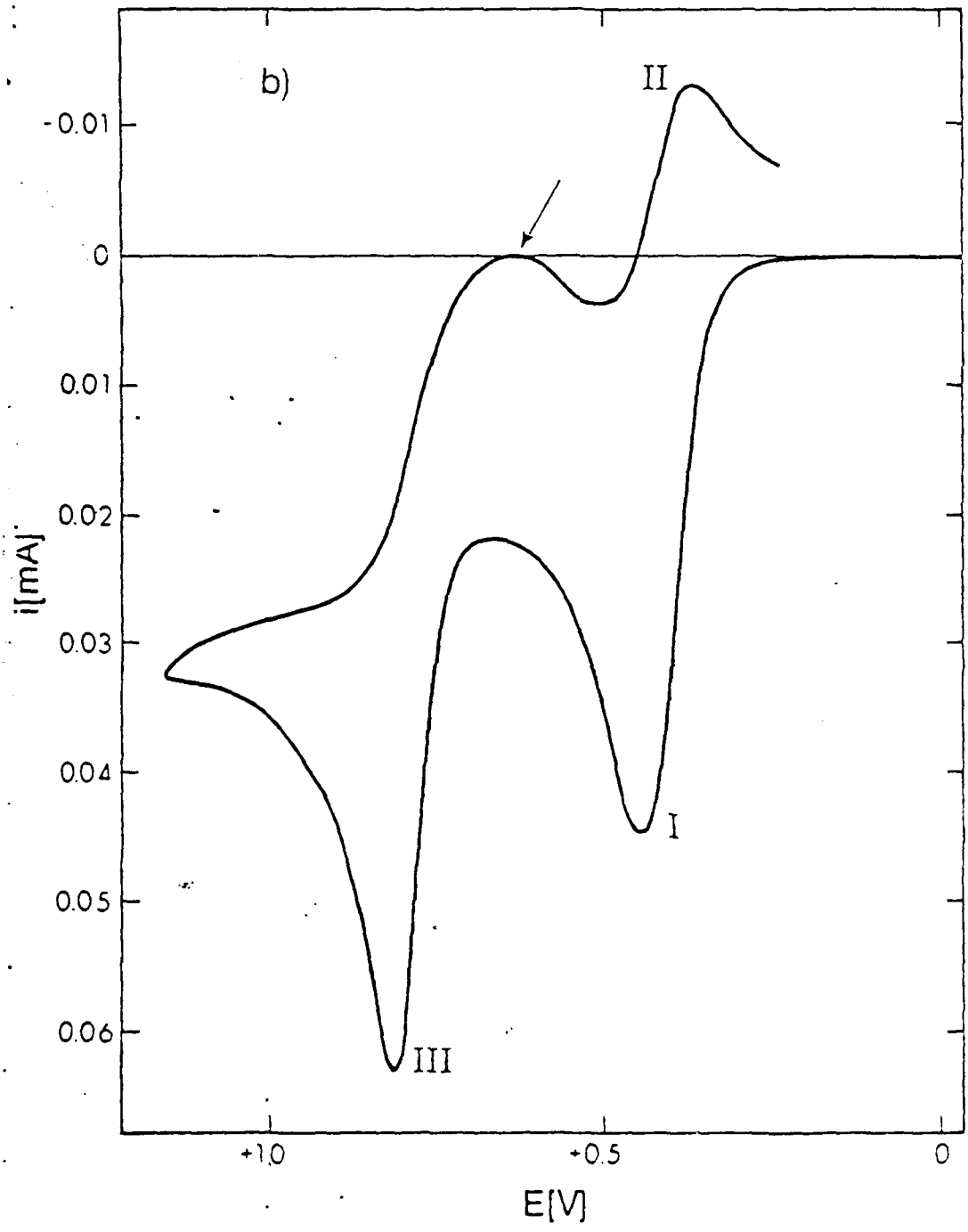
b)
II
I
III
-0.01
0
0.01
0.02
0.03
0.04
0.05
0.06
i[mA]
+1.0
+0.5
0
E[V]

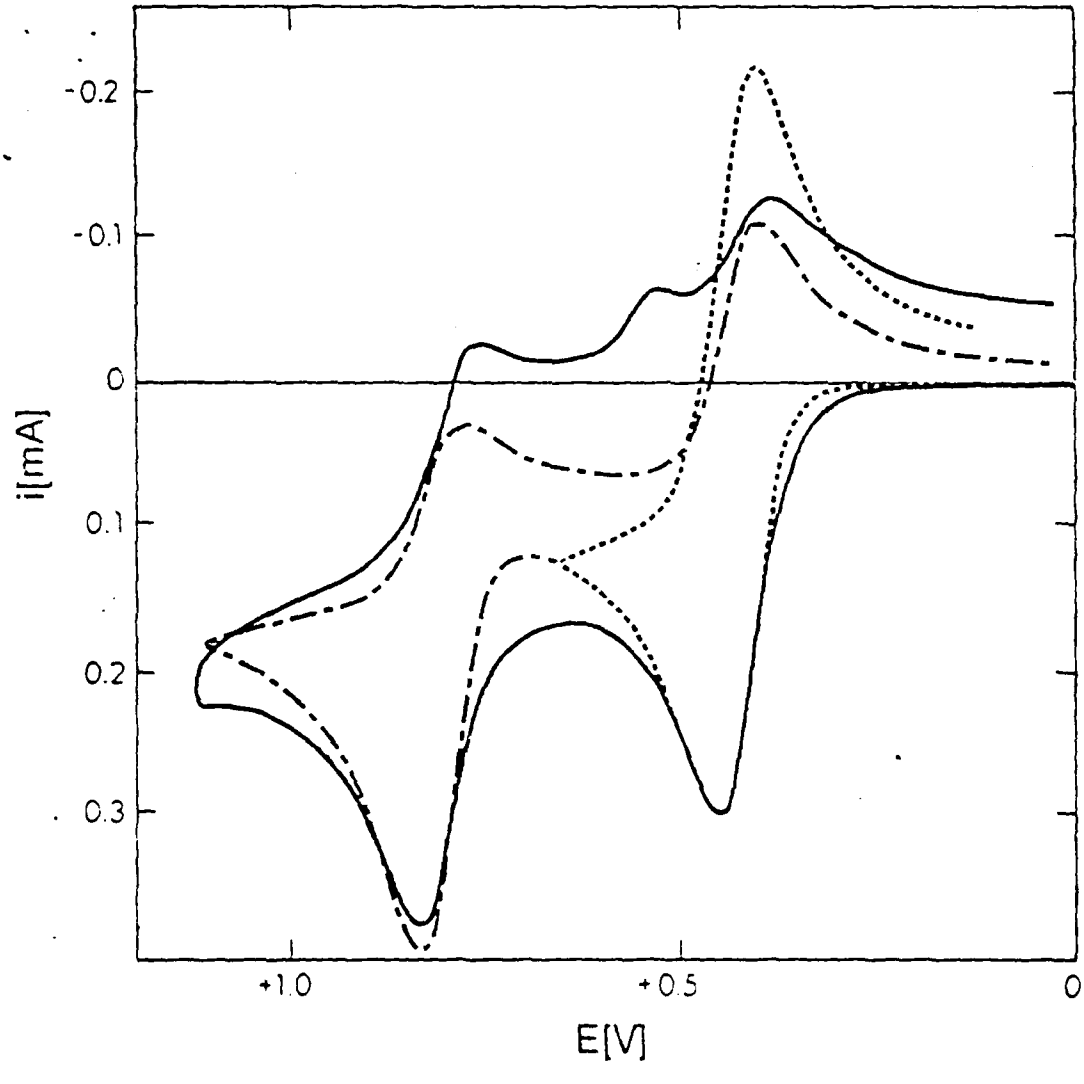
-0.2
-0.1
0
0.1
0.2
0.3
i[mA]
+1.0
+0.5
0
E[V]

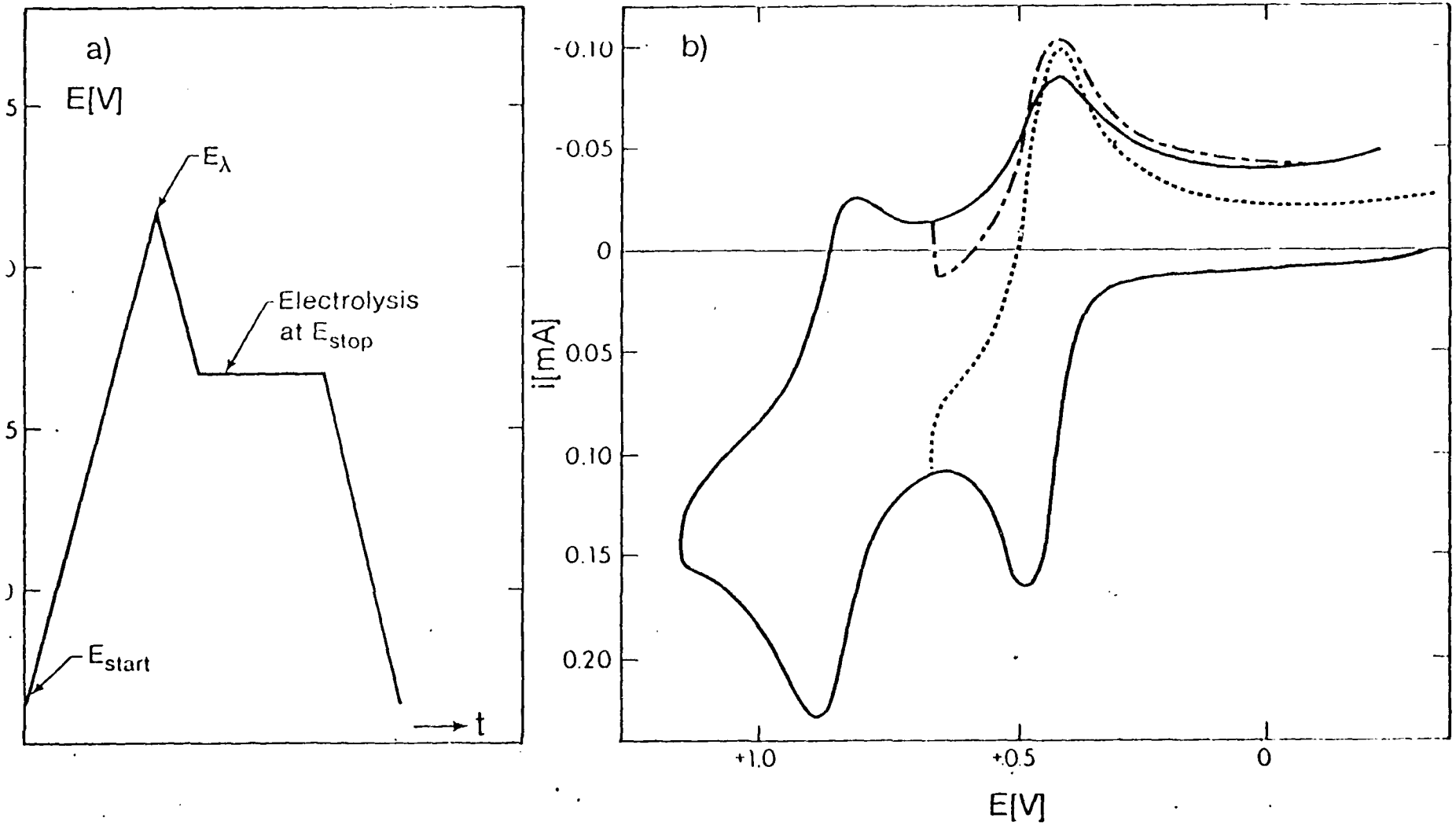
a)
E[V]
E_λ
Electrolysis
at E_{stop}
E_{start}
t
b)
-0.10
-0.05
0
0.05
0.10
0.15
0.20
i[mA]
+1.0
+0.5
0
E[V]

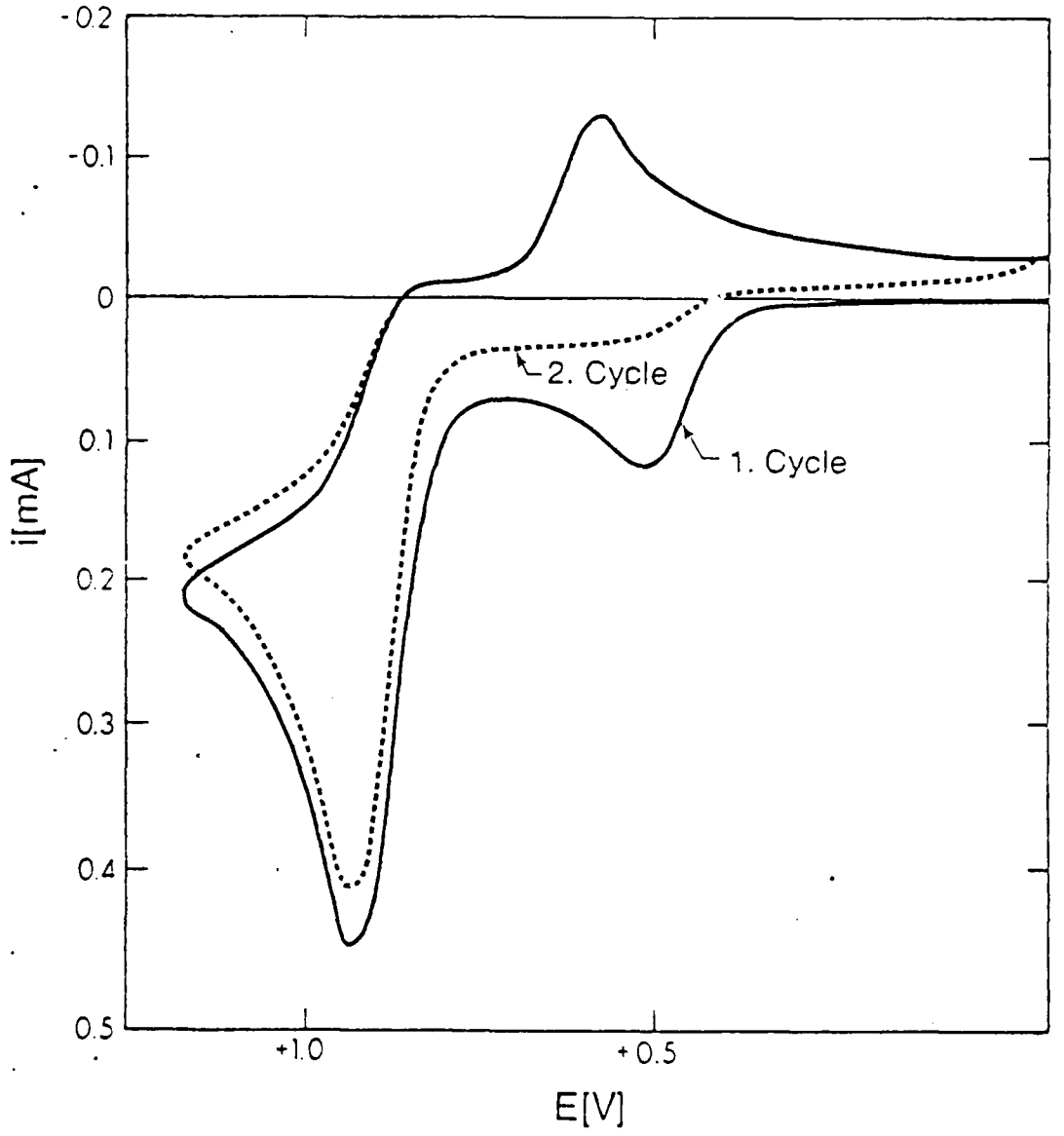
-0.2
-0.1
0
0.1
0.2
0.3
0.4
0.5
i[mA]
2. Cycle
1. Cycle
+1.0
+0.5
E[V]

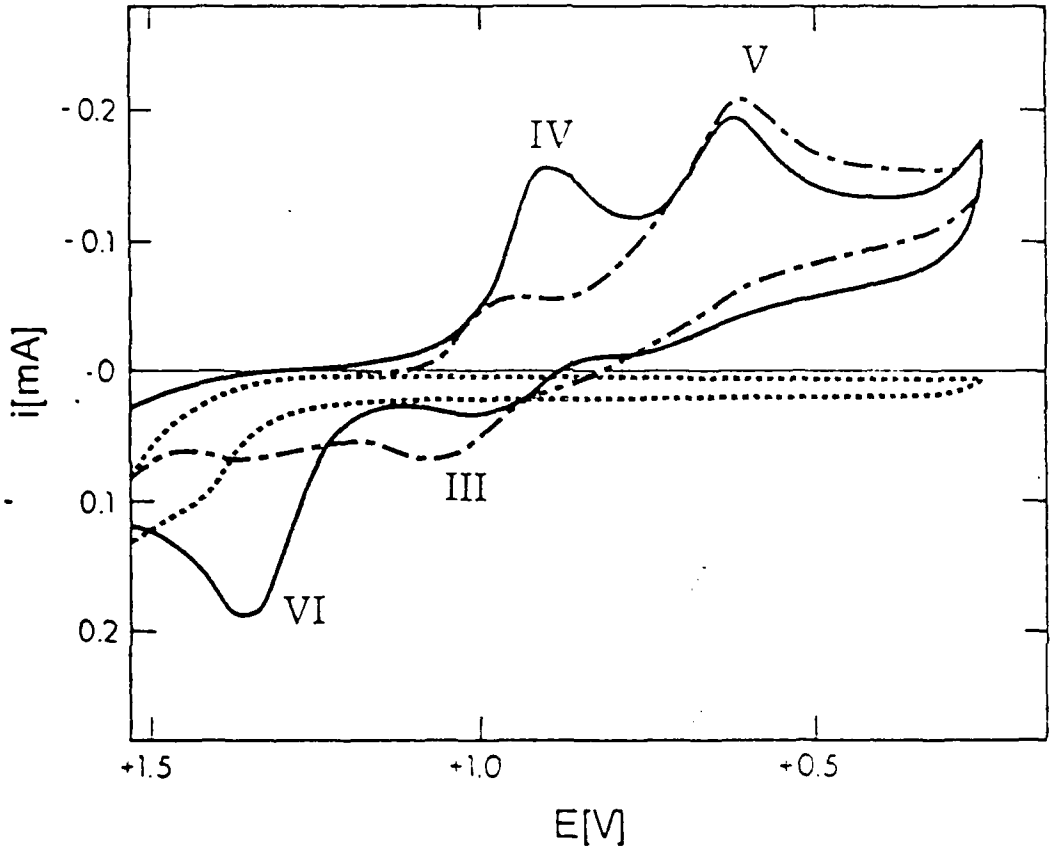
V
IV
III
VI
-0.2
-0.1
-0
0.1
0.2
i[mA]
+1.5
+1.0
+0.5
E[V]

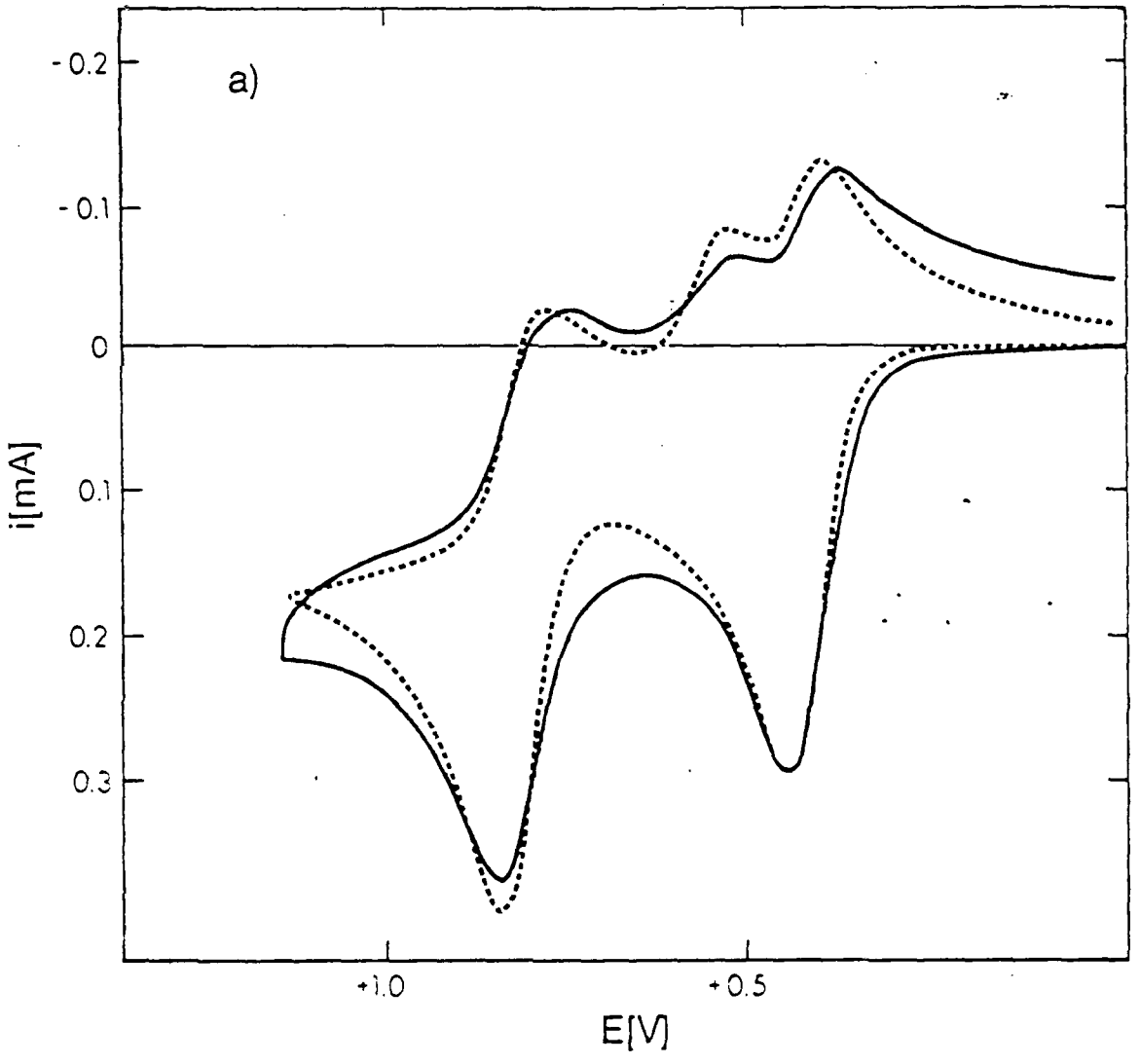
a)
-0.2
-0.1
0
0.1
0.2
0.3
i[mA]
+1.0
+0.5
E[V]

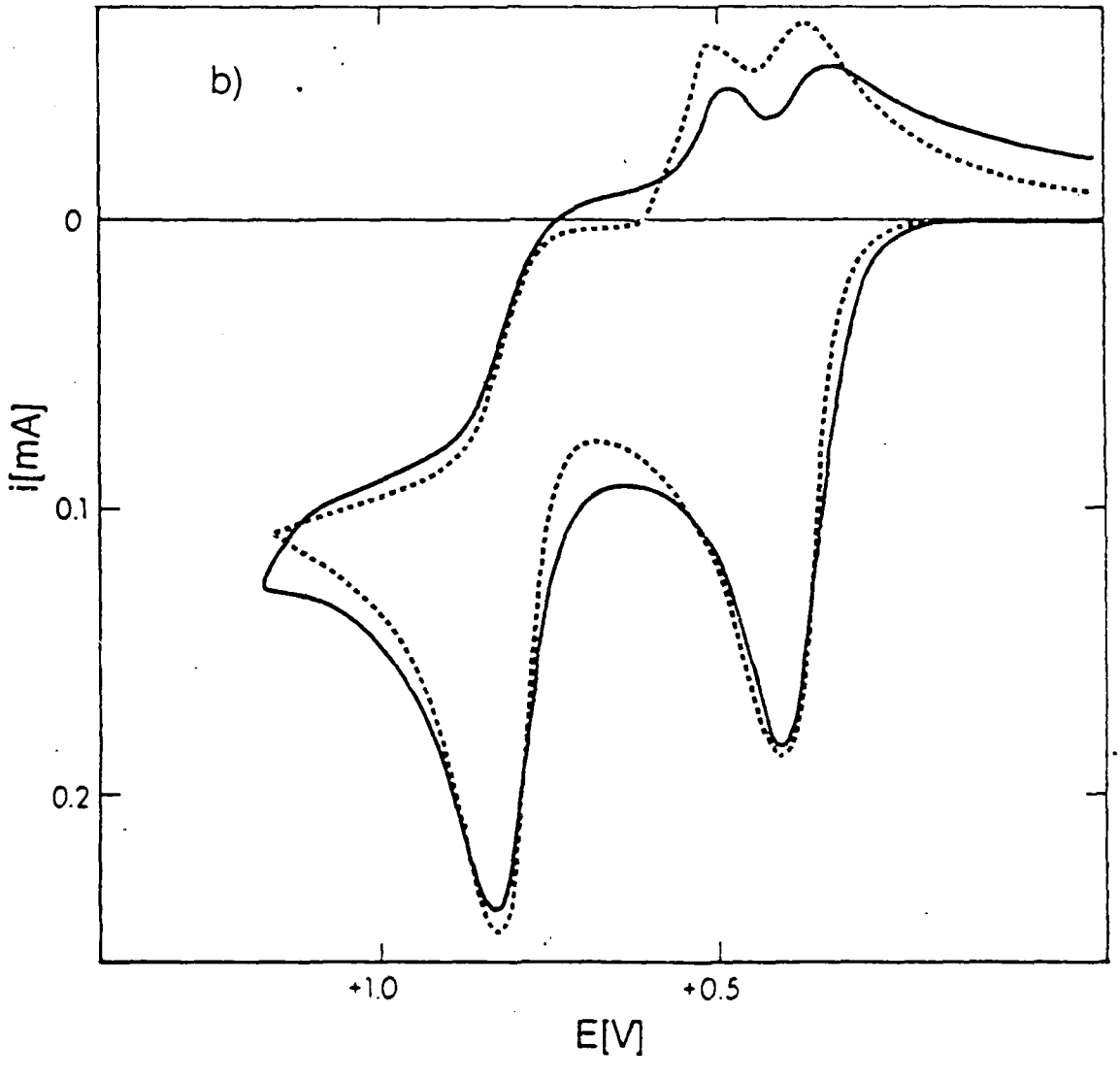
b)
0
0.1
0.2
i[mA]
+1.0
+0.5
E[V]

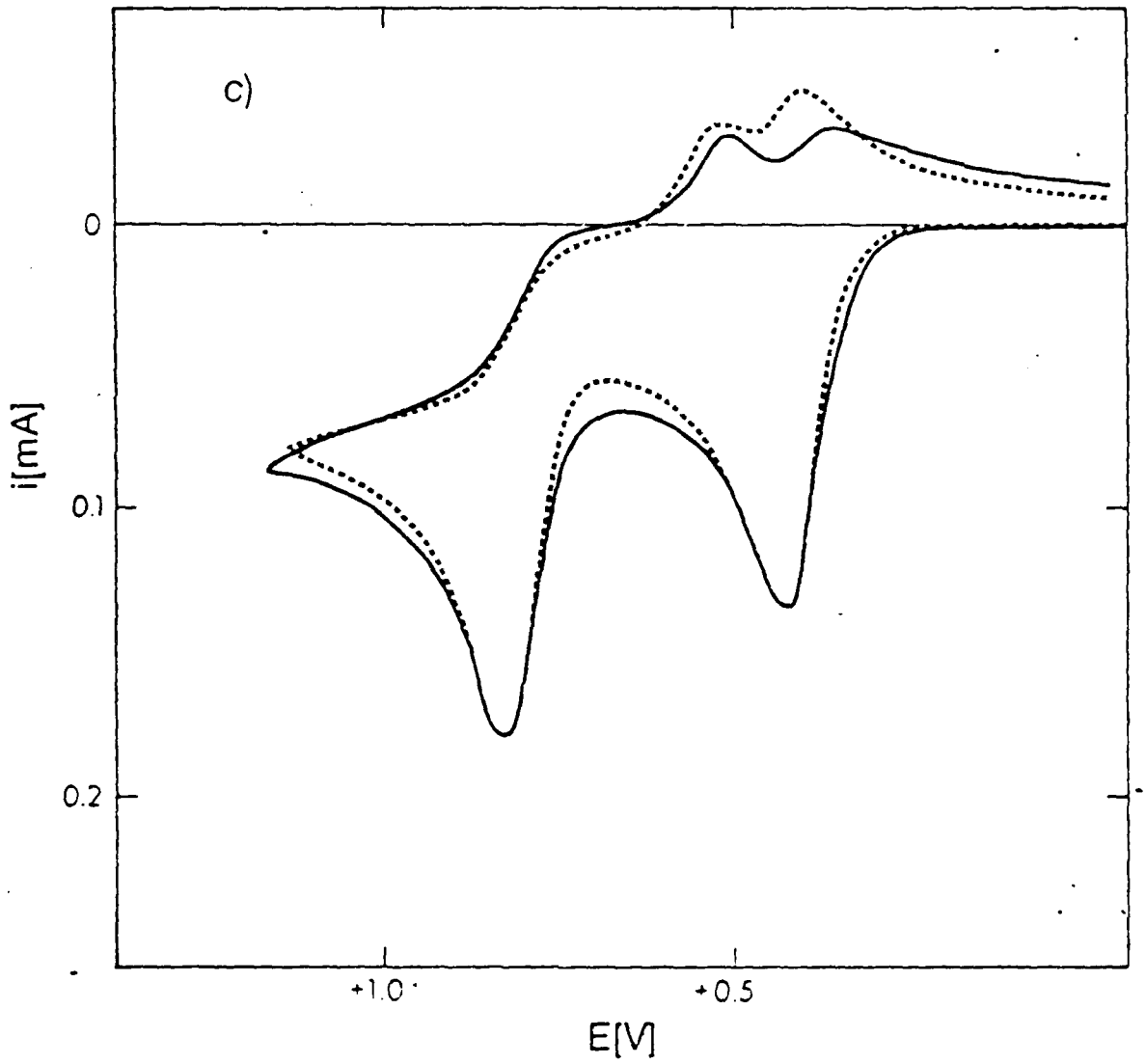
c)
0
0.1
0.2
i[mA]
+1.0
+0.5
E[V]

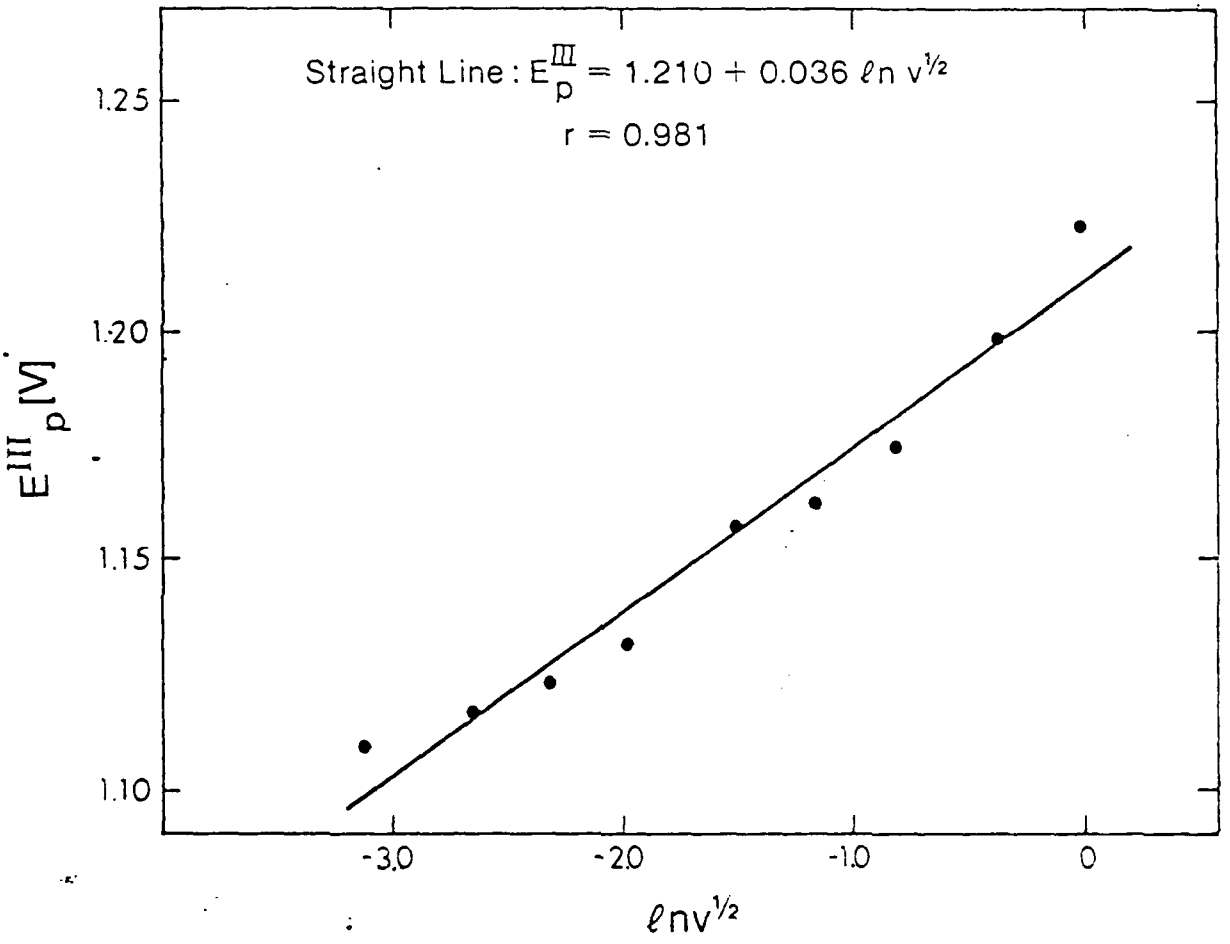
Straight Line : $E_p^{III} = 1.210 + 0.036\ \ell n\ v^{1/2}$
r = 0.981
1.25
1.20
1.15
1.10
E^{III}_p[V]
-3.0
-2.0
-1.0
0
$\ell nv^{1/2}$

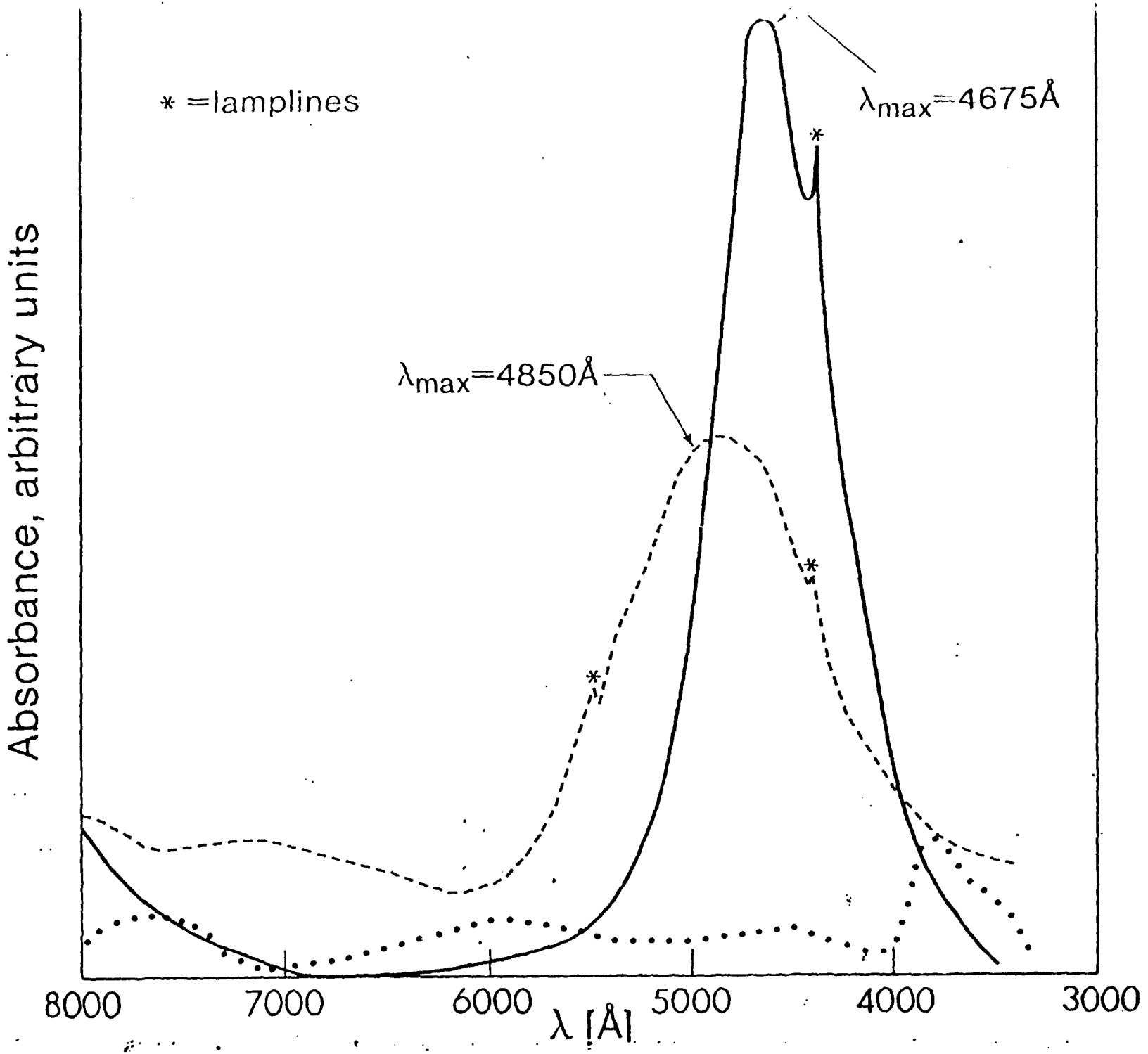
* =lamplines
λmax=4675Å
λmax=4850Å
Absorbance, arbitrary units
8000
7000
6000
5000
4000
3000
λ [Å]

APPENDIX

The mechanism for the oxidation of aniline 1b may be described by the following model, where A stands for 1b, B for 2b, C for 3b, D for 6b, HA^+ for 7b, $HA^{\cdot++}$ for 8b, E for 5b and P_1 and P_2 for products of chemical reactions of the nitrenium ion and the radical cation:

$$A \rightleftarrows B \qquad E^\circ_{A/B},\ n_1 \qquad (A1)$$

$$B \rightleftarrows C \qquad E^\circ_{B/C},\ n_2 \qquad (A2)$$

$$C + D + H^+ \qquad k_1 \qquad (A3)$$

$$A + H^+ \rightleftarrows AH^+ \qquad k_2,\ K_2 = k_2/k_{-2} \qquad (A4)$$

$$HA^+ \rightleftarrows HA^{\cdot++} \qquad E^\circ_{HA^+/HA^{\cdot++}},\ n_3 \qquad (A5)$$

$$HA^{\cdot++} + B + H^+ \qquad k_3 \qquad (A6)$$

$$D + P_1 + H^+ \qquad k_4 \qquad (A7)$$

$$E \rightleftarrows D \qquad E^\circ_{E/D},\ n_4 \qquad (A8)$$

$$2E + H^+ + D + A \qquad k_5 \qquad (A9)$$

$$B + P_2 \qquad k_6 \qquad (A10)$$

Reaction (A10) does not necessarily have to be included here because we do not see this reaction in our experiments. For the simulation k_6 has been set to zero.

We can formulate the kinetic diffusion equations for this model by

$$\frac{\partial c_A}{\partial t} = D\frac{\partial^2 c_A}{\partial x^2} - k_2 c_A c_{H^+} + k_{-2} c_{HA^+} + k_5 c_E c_{H^+} \tag{A11}$$

$$\frac{\partial c_B}{\partial t} = D\frac{\partial^2 c_B}{\partial x^2} + k_3 c_{HA^{\cdot ++}} - k_6 c_B \tag{A12}$$

$$\frac{\partial c_C}{\partial t} = D\frac{\partial^2 c_C}{\partial x^2} - k_1 c_C \tag{A13}$$

$$\frac{\partial c_D}{\partial t} = D\frac{\partial^2 c_D}{\partial x^2} + k_1 c_C - k_4 c_D + k_5 c_E c_{H^+} \tag{A14}$$

$$\frac{\partial c_E}{\partial t} = D\frac{\partial^2 c_E}{\partial x^2} - 2k_5 c_E c_{H^+} \tag{A15}$$

$$\frac{\partial c_{H^+}}{\partial t} = D\frac{\partial^2 c_{H^+}}{\partial x^2} + k_1 c_C - k_2 c_A c_{H^+} + k_3 c_{HA^{\cdot ++}} - k_5 c_E c_{H^+} + k_4 c_D + k_{-2} c_{HA^+} \tag{A16}$$

$$\frac{\partial c_{HA^+}}{\partial t} = D\frac{\partial^2 c_{HA^+}}{\partial x^2} + k_2 c_A c_{H^+} - k_{-2} c_{HA^+} \tag{A17}$$

$$\frac{\partial c_{HA^{\cdot ++}}}{\partial t} = D\frac{\partial^2 c_{HA^{\cdot ++}}}{\partial x^2} - k_3 c_{HA^{\cdot ++}} \tag{A18}$$

(where the reaction between E and H^+ has been formulated as a second order reaction, which gave better agreement with the experiment). The model is subject to the following initial (A19) and boundary (A20-A30b) conditions:

$$x > 0,\ t = 0: \quad c_A = c_A^0,\ c_B = c_C = c_D = c_E = c_{H^+} = c_{HA^+} = c_{HA^{\cdot++}} = 0 \tag{A19}$$

$$x \to \infty,\ t > 0: \quad c_A \to c_A^0,\ c_B = c_C = c_D = c_E = c_{H^+} = c_{HA^+} = c_{HA^{\cdot++}} \to 0 \tag{A20}$$

$$x = 0,\ t > 0: \quad \left(\frac{\partial c_A}{\partial x}\right)_{x=0} = -\left[\left(\frac{\partial c_B}{\partial x}\right)_{x=0} + \left(\frac{\partial c_C}{\partial x}\right)_{x=0}\right] \tag{A21}$$

$$\left(\frac{\partial c_E}{\partial x}\right)_{x=0} = -\left(\frac{\partial c_D}{\partial x}\right)_{x=0} \tag{A22}$$

$$\left(\frac{\partial c_{HA^+}}{\partial x}\right)_{x=0} = -\left(\frac{\partial c_{HA^{\cdot++}}}{\partial x}\right)_{x=0} \tag{A23}$$

$$\left(\frac{\partial c_{H^+}}{\partial x}\right)_{x=0} = 0 \tag{A24}$$

$$c_A/c_B = \Theta_{A/B}\, S_\lambda(t) \tag{A25}$$

$$c_B/c_C = \Theta_{B/C}\, S_\lambda(t) \tag{A26}$$

$$c_E/c_D = \Theta_{E/D}\, S_\lambda(t) \tag{A27}$$

$$c_{HA^+}/c_{HA^{\cdot++}} = \Theta_{HA^+/HA^{\cdot++}}\, S_\lambda(t) \tag{A28}$$

where

$$\Theta_{X/Y} = \exp\left[\frac{nF}{RT}(E^0_{X/Y} - E_{start})\right] \quad (A29)$$

and for $n_1 = n_2 = n_3 = n_4 = n$

$$S_\lambda(t) = \begin{cases} \exp(-at) & (A30a) \\ \exp(at - 2at_\lambda) & (A30b) \end{cases}$$

These equations and conditions have to be transformed into dimensionless expressions [11,12] using

$$T' = at = \frac{nFv}{RT} t \quad (A31)$$

$$X = x/L \quad (A32)$$

$$c_X^* = c_X/c_A^0 \quad (A33)$$

$$\delta = D/aL^2 \quad (A34)$$

$$\alpha_i = k_i/a \text{ for } i = 1, 3, 4, 6 \quad (A35a)$$

$$\alpha_i = k_i c_A^0/a \text{ for } i = 2, 5 \quad (A35b)$$

Discretization of the spatial coordinate finally gives a system of ordinary differential equations (A36)-(A43) (for details see [11]) which can be integrated easily:

$$\left.\frac{dc_A^*}{dT'}\right|_{X_i} = \beta\{-\frac{B_{i,1}\Theta_{A/B}\Theta_{B/C}S_\lambda(T')^2}{A_{1,1}[1+\Theta_{B/C}S_\lambda(T')+\Theta_{A/B}\Theta_{B/C}S_\lambda(T')^2]} \times$$

$$[A_{1,N+2}+\sum_{j=2}^{N+1}A_{1,j}[c_A^*(X_j,T')+c_B^*(X_j,T')+c_C^*(X_j,T')]]$$

$$+B_{i,N+2}+\sum_{j=2}^{N+1}B_{i,j}c_A^*(X_j,T')\}-\alpha_2 c_A^* c_H^*+ \qquad (A36)$$

$$\left.\frac{dc_B^*}{dT'}\right|_{X_i} = \beta\{-\frac{B_{i,1}\Theta_{B/C}S_\lambda(T')}{A_{1,1}[1+\Theta_{B/C}S_\lambda(T')+\Theta_{A/B}\Theta_{B/C}S_\lambda(T')^2]} \times$$

$$[A_{1,N+2}+\sum_{j=2}^{N+1}A_{1,j}[c_A^*(X_j,T')+c_B^*(X_j,T')+c_C^*(X_j,T')]]$$

$$+\sum_{j=2}^{N+1}B_{i,j}c_B^*(X_j,T')\}+\alpha_3 c_{HA}^{*++}-\alpha_6 c_B^* \qquad (A37)$$

$$\left.\frac{dc_C^*}{dT'}\right|_{X_i} = \beta\{-\frac{B_{i,1}}{A_{1,1}[1+\Theta_{B/C}S_\lambda(T')+\Theta_{A/B}\Theta_{B/C}S_\lambda(T')^2]} \times$$

$$[A_{1,N+2}+\sum_{j=2}^{N+1}A_{1,j}[c_A^*(X_j,T')+c_B^*(X_j,T')+c_C^*(X_j,T')]]$$

$$+\sum_{j=2}^{N+1}B_{i,j}c_C^*(X_j,T')\}-\alpha_1 c_C^* \qquad (A38)$$

$$\left.\frac{dc_D^*}{dT'}\right|_{X_i} = \beta\{-\frac{B_{i,1}}{A_{1,1}[1+\Theta_{E/D}S_\lambda(T')]}\sum_{j=2}^{N+1}A_{1,j}[c_D^*(X_j,T')+c_E^*(X_j,T')]$$

$$+\sum_{j=2}^{N+1}B_{i,j}c_D^*(X_j,T')\}+\alpha_1 c_C^*-\alpha_4 c_D^*+\alpha_5 c_E^* c_H^*- \qquad (A39)$$

$$\left.\frac{dc_E^*}{dT'}\right|_{X_i} = \beta\{-\frac{B_{i,1}\Theta_{E/D}S_\lambda(T')}{A_{1,1}[1+\Theta_{E/D}S_\lambda(T')]}\sum_{j=2}^{N+1}A_{1,j}[c_D^*(X_j,T')+c_E^*(X_j,T')]$$

Table 1: Cyclic voltammetric data[a] for the second oxidation wave of 1b and 1c.

	E_p^{III} [V]	E_p^{IV} [V]	$\Delta E_p^{III/IV}$ [V]	$E^\circ(III/IV)$ [V]
1b[b]	0.90 ± 0.02	0.82 ± 0.01	0.08 ± 0.01	+0.86 ± 0.02
1c	0.38 ± 0.02	0.32 ± 0.02	0.056 ± 0.005	+0.35 ± 0.02

[a] Mean values from several experiments with different concentrations, averaged over all v and c.

[b] $v > 0.1$ [V/s].

FIGURE LEGENDS

Figure 1: Cyclic voltammograms of anilines 1a - c at platinum in acetonitrile; a) 1a, v = 0.5 V/s, 1.3 mM; b) 1b, v = 0.5 V/s, c = 1.5 mM, c) 1c, (___) experimental voltammogram v = 0.05 V/s, c = 1.5 mM, (---) simulated voltammogram, EE mechanism, simulation parameters: E°_1 = +0.162 V, E°_2 = +0.356 V, $n_1=n_2=1$.

Figure 2: Cyclic voltammograms of 1b, a) c = 1.5 mM, v = 0.05 V/s; b) v = 0.01 V/s, the arrow indicates the occurrence of proton barrier effects (see text).

Figure 3: Cyclic voltammogram of 1b in CH_2Cl_2; c = 0.97 mM, v = 0.05 V/s.

Figure 4: Experimental cyclic voltammogram of 1b [__, conditions as in Figure 1b] and simulated voltammograms of an EEC mechanism (-.-.- simulation parameters: E° = +0.407 V, E°_1 = +0.407 V, E°_2 = +0.650 V, $n_1=n_2=1$, k= 2 s^{-1}) and a reversible electron transfer (..., simulation parameters: E° = +0.407 V, E_λ = +0.650 V, n = 1).

Figure 5: Experiment to show that a reaction preventing oxidation of 1b for a certain time occurs in peak III. a) potential-time program; b) (...) cyclic voltammogram of 1b, E_λ = +0.650 V; (___) cyclic voltammogram of 1b, E_λ = +1.15 V; (-.-.-) cyclic voltammogram of 1b with electrolysis according to the potential-time program in Figure 5a); v = 0.5 V/s, c = 0.82 mM.

Figure 6: Cyclic voltammogram of a solution containing 1b and 7b; v = 0.2 V/s.

Figure 7: Cyclic voltammograms of iminoquinole 11b in CH_3CN: (...) without acid; (-.-.-) after addition of 30 µl of HBF_4 (54% in diethyl ether), (___) after addition of 530 µl of HBF_4 (54% in diethyl ether); c (11b) = 1.3 mM.

Figure 8: Experimental (___) and simulated (...) cyclic voltammograms of 1b; experimental parameters as in Figure 1b; simulation parameters are given in the text; a) v = 0.5 V/s, b) v = 0.2 V/s, c) 0.1 V/s.

Figure 9: Variation of E_p^{III} in cyclic voltammograms of 1a with ln $v^{1/2}$; the points represent mean values from seven independent experiments with different concentrations of 1a.

Figure 10: Uv/vis MSRS results for the oxidation of 1a-c in the second wave; (...) 1a, (---) 1b, (___) 1c, c = 1.0 mM.

Electrochemistry of Anilines II*: Oxidation to Dications, Electrochemical and uv/vis Spectroelectrochemical Investigation

by

Bernd Speiser[a,b], Anton Rieker[a] and Stanley Pons[b]

a) Institut für Organische Chemie
der Universität Tübingen
Auf der Morgenstelle 18
D-7400 Tübingen-1
Federal Republic of Germany

b) Department of Chemistry
University of Alberta
Edmonton, Alberta, Canada
T6G 2G2

*part I: see ref. 1

ABSTRACT

The electrochemical oxidation of 2,6-di-tert-butyl-4-R-anilines (R = C_6H_5, p-OCH_3-C_6H_4 and p-$N(CH_3)_2$-C_6H_4) at the potentials of the second peak has been investigated. Dications could be observed and characterized by electroanalytical and spectroelectrochemical means. The cyclic voltammogram of the methoxy compound has been simulated by the orthogonal collocation method. Products of bulk electrolysis have been identified. We found two different sites of attack in the case of the methoxy compound.